AD_____

Award Number: W81XWH-08-2-0139

TITLE: Mission Connect Mild TBI Translational Research Consortium

PRINCIPAL INVESTIGATOR:
Jose Perez-Polo, Ph.D.
Claire E. Hulsebosch, Ph. D.
Douglas S. Dewitt, Ph. D.

CONTRACTING ORGANIZATION: University of Texas Medical Branch, Galveston, Texas, 77555-1072

REPORT DATE: August 2013

TYPE OF REPORT: Annual

PREPARED FOR: U.S. Army Medical Research and Materiel Command
Fort Detrick, Maryland 21702-5012

REPORT DOCUMENTATION PAGE

Form Approved
OMB No. 0704-0188

1. REPORT DATE	**2. REPORT TYPE**	**3. DATES COVERED**
August 2013	Annual	1 August 2012- 31 July 2013

4. TITLE AND SUBTITLE
Mission Connect Mild TBI Translational Research Consortium

5a. CONTRACT NUMBER

5b. GRANT NUMBER
W81XWH-08-2-0139

5c. PROGRAM ELEMENT NUMBER

6. AUTHOR(S)
Jose Perez-Polo, Claire E. Hulsebosch; Douglas S. DeWitt

E-Mail: Regino.perez-polo@utmb.edu

5d. PROJECT NUMBER

5e. TASK NUMBER

5f. WORK UNIT NUMBER

7. PERFORMING ORGANIZATION NAME(S) AND ADDRESS(ES)
University of Texas Medical Branch,
Galveston,TX, 77555-1072

8. PERFORMING ORGANIZATION REPORT NUMBER

9. SPONSORING / MONITORING AGENCY NAME(S) AND ADDRESS(ES)
U.S. Army Medical Research and Materiel Command
Fort Detrick, Maryland 21702-5012

10. SPONSOR/MONITOR'S ACRONYM(S)

11. SPONSOR/MONITOR'S REPORT NUMBER(S)

12. DISTRIBUTION / AVAILABILITY STATEMENT
Approved for Public Release; Distribution Unlimited

13. SUPPLEMENTARY NOTES

14. ABSTRACT
Mild traumatic brain injury (mTBI), such as mild "blast" injuries due to improvised exploding devices, result in long term impairment of cognition and behavior. Our hypothesis is that there are inflammatory outcomes to mTBI over time that cause pathogenesis and clinical outcomes. We used an adaptation of rat moderate brain lateral fluid percussion (LFP) brain injury and compared 2 blast models developed by us. We characterized a rat mild blast brain injury model (mBBI) that increased IL-1β and TNFα levels, macrophage/microglial and astrocytic activation, and blood brain barrier disruption. We assessed beneficial outcomes after blockade of the IL-1α/β and TNFα receptors in the mLFP brain injury model. We found that blocking the IL-1α/β and TNFR receptors, singly or in combination, with wo FDA-approved drugs (Kineret or Interleukin-1 Receptor Antagonist, IL-1Ra and Etanercept or antibody to the Tumor Necrosis Factor Receptor improved outcomes by ameliorating inflammation. We also determined an optimal time course of treatment. We also characterized our selected mBBI model of mTBI, the Vanderberg model. We found similar resulting righting reflex response times (RRRT) for the mBBI as compared to the mLFP injury. We determined that there were significant increases in IL-1β and TNFα levels, macrophage/microglial and astrocytic activation, and phosphorylated Tau (p-Tau) levels, the latter indicative of neuroencephalopathy, in the injured cortex, hippocampus, thalamus and amygdala. Whereas there was an apparent correlation between the RRRT values and the p-Tau levels, general inflammatory responses were more threshold-triggered. These results suggest potential therapies for mild blast injuries.

15. SUBJECT TERMS- Blast head injury; mild head injury; anti-inflammatory therapy; cytokine receptors; IL-1; TNFα; encephalopathy

16. SECURITY CLASSIFICATION OF:			**17. LIMITATION OF ABSTRACT**	**18. NUMBER OF PAGES**	**19a. NAME OF RESPONSIBLE PERSON**
a. REPORT	**b. ABSTRACT**	**c. THIS PAGE**			USAMRMC
U	U	U	UU		**19b. TELEPHONE NUMBER** *(include area code)*

Table of Contents

Page

INTRODUCTION

Midl traumatic brain injuries (**mTBI**) are common among our military personnel (Hogue et al., 2008; Kamnash et al., 2012) and mild blast brain injuries (**mBBI**) are responsible for over 80% of casualties in the last decade (Levin et al., 2010). Mild "blast" injuries due to improvised exploding devices have long term cognitive and behavioral deficits (Cantu, 2007; Dept. VA and DOD, 2010; Okie, 2005; Omalu, 2005; 2006). Rat models of mTBI have shown an important role for cortex, hippocampus, thalamus and amygdala as evidenced by the resultant neuropathophysiology (Elder et al., 2012; Perez-Polo et. al., 2013). A clinical outcome of these neuronal and glial losses could be the long term **encephalopathy** frequently documented years after a TBI incident or incidents (Cantu, 2007; Omalu et al., 2006). Both for injured athletes and blast TBI rodent models, there are documented increases in the levels of phosphorylated Tau protein (**p-Tau**) **taupathy** associated with significant encephalopathy (McKee et al., 2009). Although for moderate and severe TBI, it is known that the resultant vascular dysruption and triggered inflammatory cascades result in cell death and neuronal dysfunction (Israelsson et al., 2008; Donkin et al., 2009); less is known about its "mild" form. Our **first** goal was to select models that fit many of the clinical issues as a useful tool to increase our understanding of the role of inflammation in mTBI that at the same time provides a platform for the development and assessment of intervention strategies that will lead to clinical therapies relevant to the military theatre. A **second** goal has been to test two FDA-approved drugs in a pre-clinical context consistent with battlefield conditions. We have shown that for mild lateral fluid percussion (mLFP) injury there are increased levels of Interleukin 1 (**IL-1**) and Tumor Necrosis Factor alpha (**TNFα**) followed by blood brain barrier impairment and increased inflammation that may be responsible for the observed neuronal losses in the aforementioned brain areas. We hypothesize that blocking the IL-1 receptor with Kineret agonist or the TNF-α receptor with its cognate antibody Etanercept will improve outcomes by ameliorating inflammation. We test these hypotheses using the mLFP model of mTBI developed by us. A **third** goal is to develop and assess a model of "mild blast" injury, the **Vandenberg** (blast brain injury or **BBI**) that is in concordance with clinical parameters and determine if the mechanistic assessments based on the stimulation of IL1β by mTBI we have performed with the mild LFP injury model are also applicable. Such a result would augment the clinical validity of our approach.

SPECIFIC AIMS

Specific Aim #3: **To develop new and innovative treatment strategies for MTBI and provide the preclinical and phase 1-2 testing of treatments found to improve outcome.**

Specific Aim #3.3: To study the role of IL-1 and TNF receptor activation in neurological deficits after TBI

Specific Aim #3.3.1: To serially measure brain cytokine levels after MTBI

Specific Aim #3.3.2: To study the role of IL-1 receptor activation in neuronal cell death and in the inflammatory response after MTBI

Specific aim #3.3.3: To study the role of TNF receptor activation in neurological deficits after TBI

Body of the Report
Progress to Date (August 1, 2012 to July 31, 2013)

Our hypotheses are that:

- mTBI resulting from a mild lateral fluid percussion brain injury (**mLFP** injury), or a mild blast injury (**mBBI**), trigger increases in inflammatory cytokines resulting in significant neuropathology as measured by cell and myelin losses; astrocytic, macrophage and microglial activation, impairment of the blood brain barrier and behavioral and cognitive impairment.
- Prompt post-injury blockade of the inflammatory cytokine receptors binding cytokines whose levels increase after mTBI with FDA-approved drugs will have beneficial effects.
- A mild blast brain injury model of mTBI, mBBI, has similar characteristics to the mLFP injury model as well as exhibits neuroencephalopathy.

Thus, given our demonstration of increased IL-1α/β and TNF-α after either mLFP injury or mBBI, we hypothesize that blocking the IL-1 receptor with Kineret agonist or the TNF-α receptor with its cognate antibody Etanercept will improve outcomes by ameliorating inflammation. Furthermore, we test these hypotheses using the mild lateral fluid percussion brain injury rodent model (mLFP) adapted by us from the literature and a Vandenberg (mild blast brain injury or mBBI) model of mTBI developed and characterized by us.

Figure 1. Specific Aim 3.3 Schematic

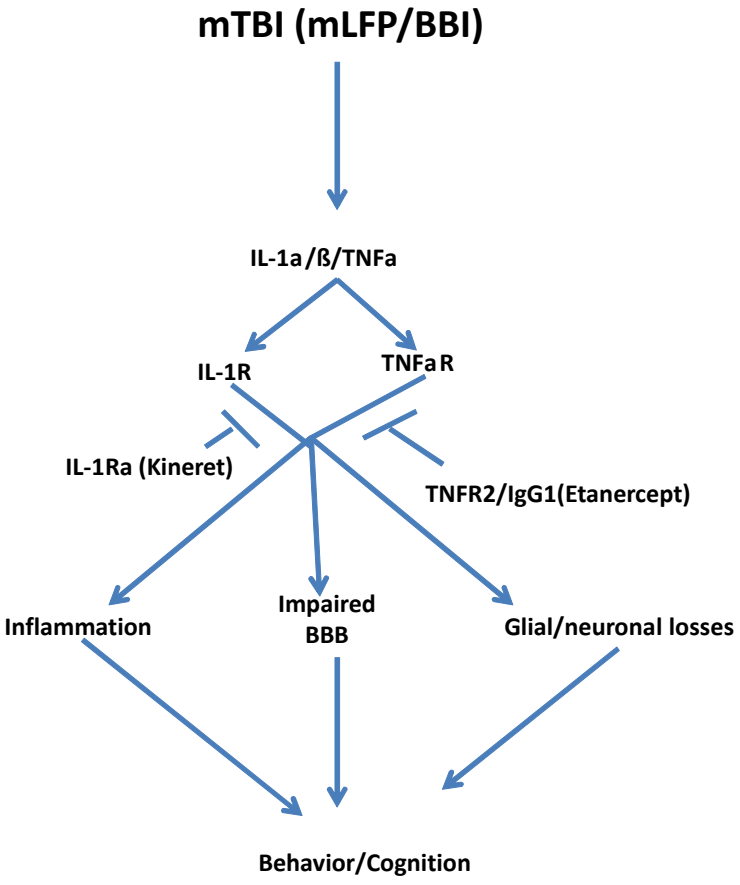

As presented in previous reports and described in Perez-Polo et al., (2013), we have shown in the mLFP injury model that the key brain inflammatory cytokine Interleukin 1 (IL-1) and Tumor Necrosis Factor alpha (TNFα) protein levels increase as early as 3 and 6 hours across several brain structures and there is a return to basal levels by 18 days post-injury, except at the injury site where there is a detectable IL-1β presence. The mLFP injury also increased acute and chronic activation of astrocytes and microglia, which were shown to be the source for the increased levels of IL-1 and TNFα. We also demonstrated the mLFP injury resulted in impairment of the blood brain barrier (BBB) as evidenced by an increased presence of blood borne proteins such as albumin and IgG as well as an in increase in the BBB dysfunctional marker SMI-71 by 6 hours post injury and that this impairment persists up to 18 days.

We also determined the ameliorative effects of both individual Kineret and Etanercept treatments as well as combined treatments on mLFP injury (see **Figure 2** for treatment protocol**).** For example, 18 days after the treatments described in **Figure 2**, there were significant ameliorations of the neuropathology observed in cortex, hippocampus, thalamus and amygdala and the behavioral deficits resulting from mLFP injury (**Figures 3-5**). Combined treatments with Kineret and Etanercept did not significantly improve the beneficial effects observed after individual treatments. Also, there were no significant improvements at 18 days compared to those observed at 6 hours, leading to the conclusion that single treatment within the first 6 hours after injury was as effective as the combined more extensive treatment protocol for 11 days described in **Figure 2**.

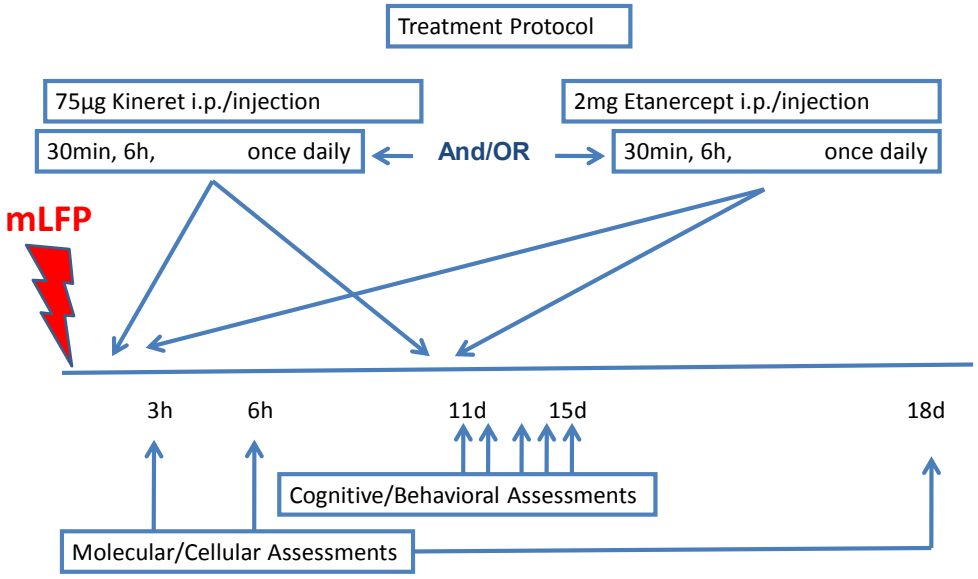

Figure 2. Treatment Protocol with Kineret and Etanercept blockade of IL-1 α/β and TNFα receptors respectively. Groups: naïve, sham, vehicle- and drug-treated.

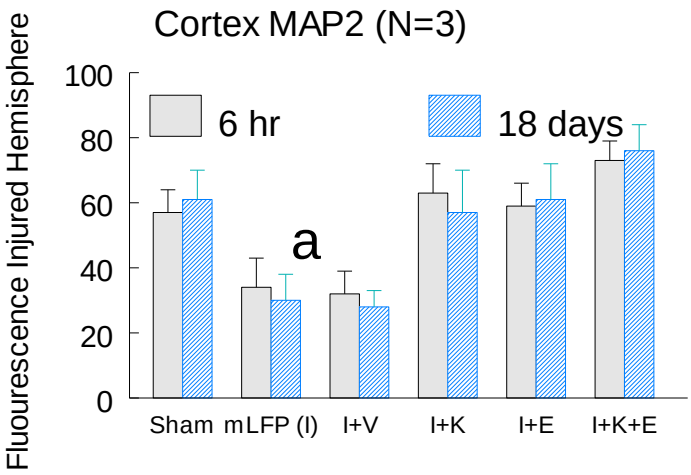

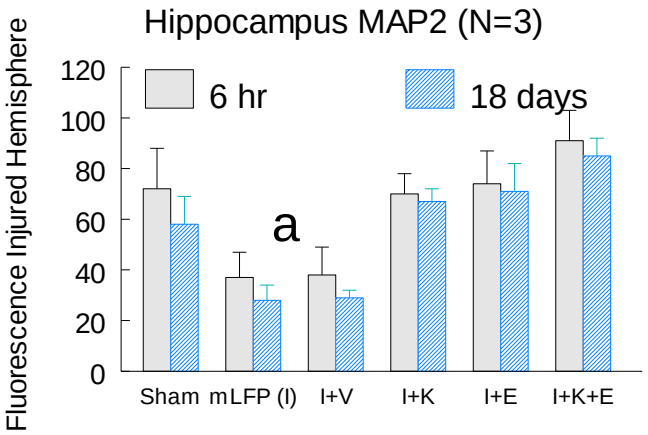

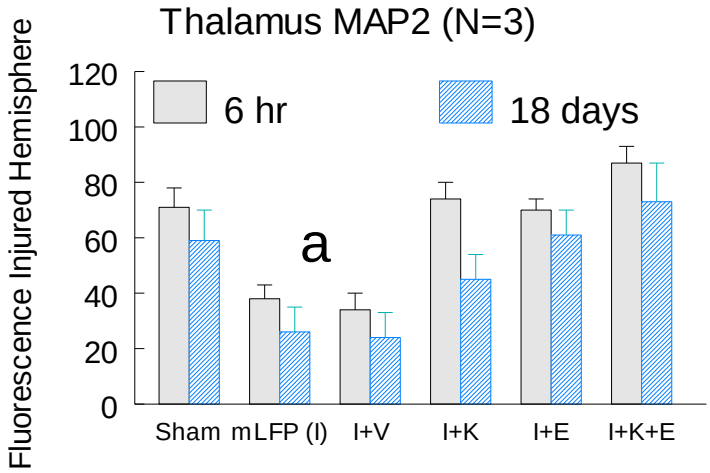

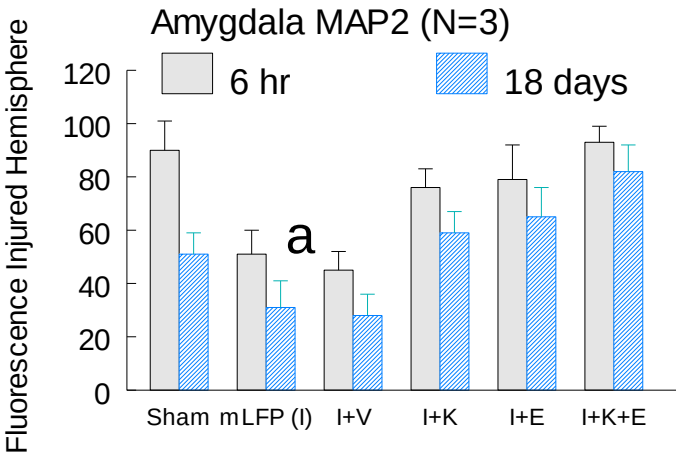

Figure 3. Quantitation of immunofluorescence 18 days after mLFP injury. (a) = p<0.01 naïve or sham vs Injury or injury + vehicle (I+V); p<0.05 Injury or I+V vs I+Kineret (I+K) or injury + Etanercept (I+E) or both (I+K+E); all other comparisons are not significant.

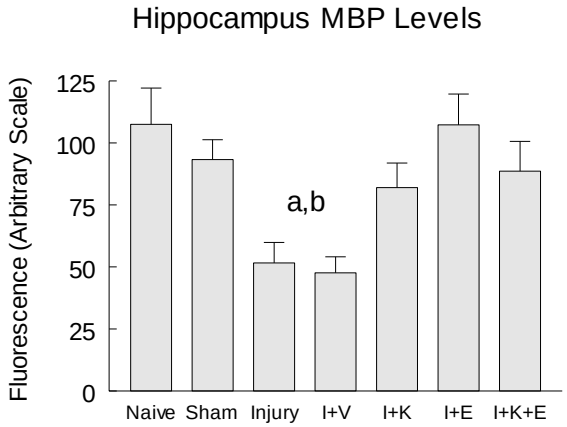

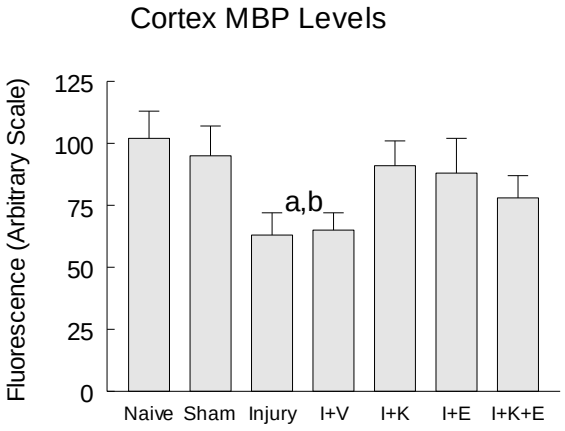

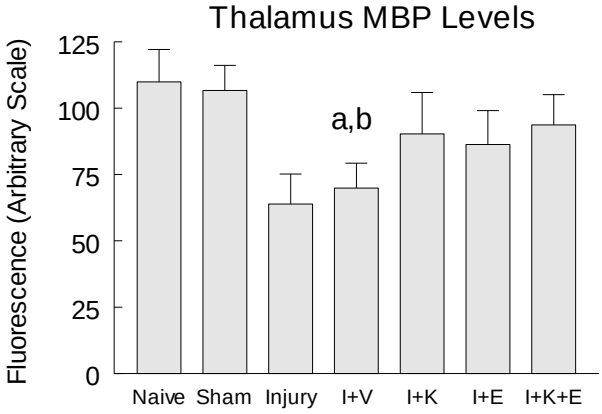

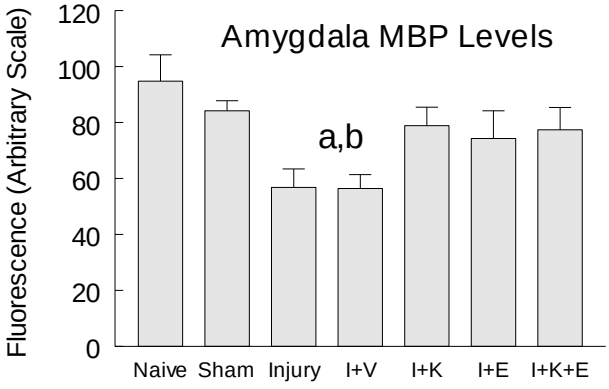

Figure 4. Quantitation of immunofluorescence 18 days after mLFP injury. (a) = p<0.01 naïve or sham vs Injury or injury + vehicle (I+V); (b) = p<0.05 Injury or I+V vs I+Kineret (I+K) or injury + Etanercept (I+E) or both (I+K+E); all other comparisons are not significant. N = 9.

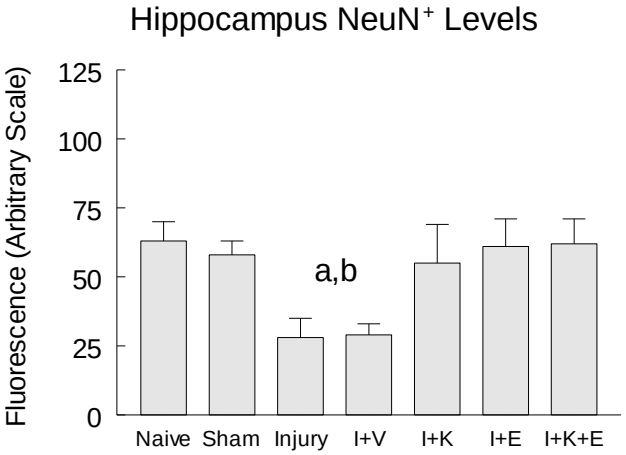

Figure 5. Working Memory Assay.

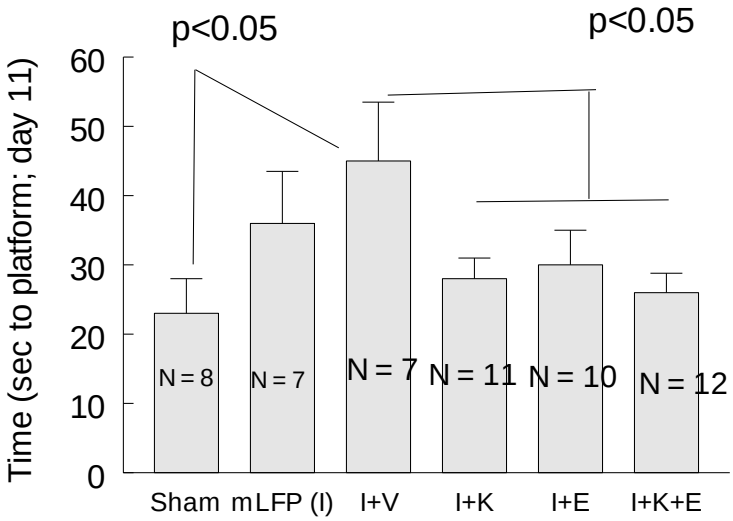

Figure 5. Effect of treatments on working memory as assessed Quantitation of immunofluorescence 18 days after mLFP injury. (a) = p<0.01 naïve or sham vs Injury or injury + vehicle (I+V); (b) = p<0.05 Injury or I+V vs I+Kineret (I+K) or injury + Etanercept (I+E) or both (I+K+E); all other comparisons are not significant.

Blast Injury

In the latter part of the year, we focused on the characterization of the Vandenberg blast brain injury device (**Figure 6**) once we showed that it provided a reliable model, at this time, of mild brain blast injury. We labeled this model **mBBI.** Understanding the mechanisms and consequences of mild TBI in our mBBI model in order to develop treatments relying on the use of FDA-approved drugs will have significant military relevance. It is clear from the reported cognitive and behavioral outcomes to mTBI due to blasts that there is likely to be involvement of the parietal cortex, hippocampus, thalamus and amygdala; our chosen immunohistological target tissues. One clinical outcome of these neuronal and glial losses could be the long term encephalopathy frequently documented years after a TBI incident or incidents (Cantu, 2007; Omalu et al., 2006). Both for injured athletes and blast TBI rodent models, there are documented increases in the levels of phosphorylated Tau protein (p-Tau) taupathy associated with significant encephalopathy (McKee et al., 2009).

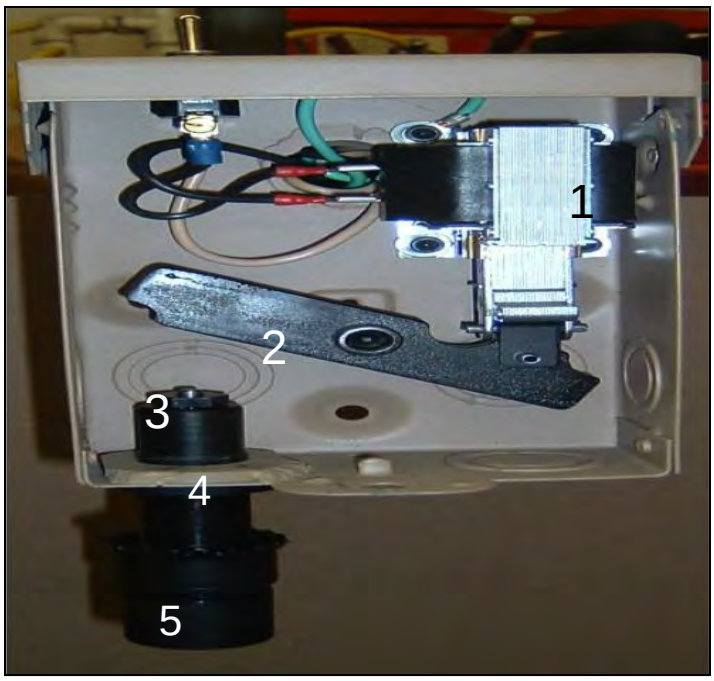

Figure 6. The Vandenberg brain blast injury apparatus uses an electric solenoid (#1) to fire blank cartridges. Force from energized solenoid is transmitted via hammer (#2) to firing pin (#3) is housed in standing breech (#4), igniting blank cartridge in the firing chamber (#5).

Our study design for mBBI (See **Figure 7**) was to expose rats to mild TBI where "mild" is defined as injury to the brain resulting in a righting reflex recovery time (**RRRT**) of anywhere from 4 to 10 minutes as compared to sham-treated animals typically showing an RRRT of between 1 and 4 minutes or moderate to severely injured animals showing an RRRT of more than 10 minutes. The mTBIs were then characterized using immunoassay arrays for cytokines, immunohistochemistry measurements of biomarkers indicative of inflammation (IBA1) and neuroencephalopathy (p-Tau). We included taupathy measurements as an index of the development of encephalopathy. We initially made our observations at 6 hours as well as at 30 days.

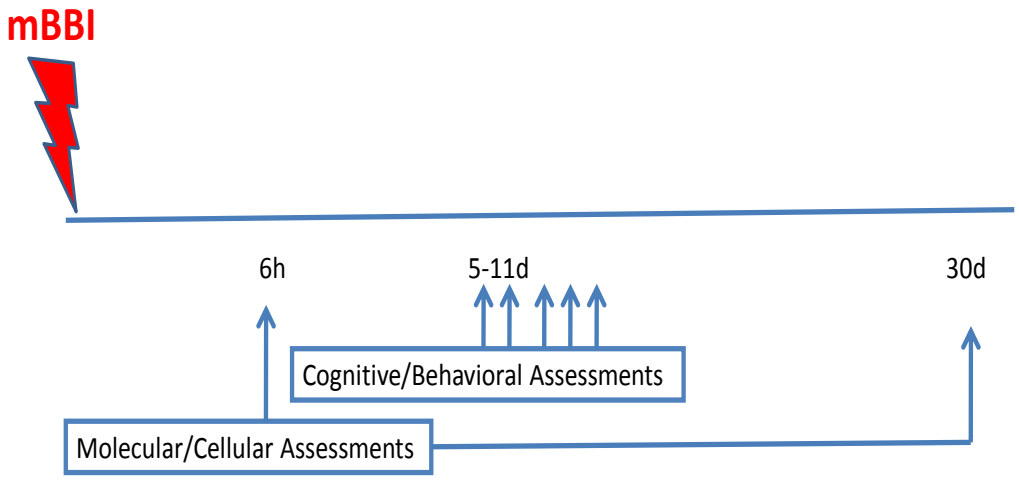

Figure 7. mBBI Protocol Groups: naïve, sham, and injured.

Rats are anesthetized with 4.0% isoflurane in an anesthetic chamber, intubated with a pediatric endotracheal tube using a custom modified pediatric laryngoscope. The rats are mechanically ventilated with 2.0% isoflurane in Medical O2:Medical air (30:70) using a volume ventilator. The rats are be prepared for blast injury by shaving the heads, plugging the external auditory canals with foam plugs and covering their heads with a silicone pad. The silicone pad transmits the blast pressure wave but protects the rats from flash burn injury. The rats are then positioned on a foam pad under the Vandenberg blast injury device (see **Figure 6**). Once the rat is positioned, all personnel except for the Research Associate who will perform the reflex testing and administer the blast injury leave the room, the isoflurane is discontinued, and when the animal exhibits a withdrawal reflex in response to a paw pinch, the rat is subjected to blast injury or sham injury.

For the acute **neurological evaluations** which are necessary to validate criteria for mTBI, rats are anesthetized with isoflurane and concussed with Vander Berg device at 2 cm, which produces a mTBI. Additional animals that are identically prepared but not injured serve as a sham-treated control group. Within 15 seconds following injury, the animals are removed from under the injury device and placed on a table for neurological assessment. A battery of tests is applied (Dixon et al., 1987), to characterize certain acute (60 minutes postinjury) neurological consequences of mechanical brain injury. The battery includes tests analogous to some motor components of the Glasgow Coma Scale allows quantification of features of the suppression of animals' responsiveness to external stimuli and relationships between durations of behavioral suppression and magnitudes of injury. This battery is derived in part from neurological scales previously developed by this group to evaluate the behavioral effects of brain injury on rats. For a mild level of injury, the righting response reflex should be around 10 minutes. After a brief postoperative recovery to ensure the general health of the rats (absence of pulmonary edema, cerebral hemorrhaging, etc.), the animals are allowed to recover. The assessment of the paw withdrawal, consists of gradual application of pressure on the hind paw until paw withdrawal occurs. Graded pressure can be applied by modified needle-nosed pliers having a 4-sq mm jaw for grasping tissue. Normally, pinches with a calibrated force of 0.2 kg/sq mm consistently elicits the paw flexion reflex. Paw flexion reflexes will be assessed at intervals of 1 minute until flexion occurred. Pressure greater than 2.0 kg/sq mm will not be applied to protect from tissue damage in the event that no flexion reflex results are observed. A more complex nonpostural somatomotor function is assessed by recording the duration of suppression of the startle response. The startle response is determined by observing the presence of any motor response to a brief, loud noise resulting from snapping a clipboard's paper holder. In normal animals, this stimulus reliably elicits a profound twitch and stiffening of the whole body. More complex postural somatomotor functions are assessed by recording the duration of suppression of the righting response. The righting response reflex is defined as the animal's ability to right itself three times consecutively after being placed on its back. After recovery of the righting response, spontaneous locomotion is evaluated by regularly placing the rat in a marked 25 × 25-cm area until the rat walks spontaneously out of the area.

Working memory test relies on the improved performance of the rat at the end of the second of four trials run on the fifth day post injury. The water maze is a 6’ diameter tank, filled to 2 cm above the invisible platform that is 4 inches diameter. The water temperature is held at 22-24 degrees. The platform is stationary through out the experiment. The tank is divided into four quadrants and stationary cues are marked on the wall in each quadrant. Before the first trial, the rat is placed on the platform for 30 seconds. The animals’ starting point is randomly chosen each day based on these quadrants, one trial is started from each quadrant. The SMART computer system is used to track and monitor the animal during the trials. After placing the animal in the water facing the wall of the tank, the handler leaves the room.

The animal is allowed two minutes to find and climb the platform and escape the water (latency to platform); he must remain on the platform for 30 seconds. If the animal does not find the platform, the handler places him on it for 30 seconds before removing him from the maze. The animals are given a four-minute rest period in a warming chamber between each trial. Rats are allowed to recover for 3 or 6 hour survival periods or 18 days at which time rats are anesthetized prior to sacrifice with 150mg/kg of Nembutal I.P. and perfused transcardially with 4% paraformaldehyde for immunohistochemistry or, if earmarked for immunoassays, they were sacrificed and the hippocampus, parietal cortex and thalamus are dissected and stored at -80°C until used.

The majority of brain tissues are stained with antibodies using the fluorescence method, except for a few selected tissue blocks that are paraffin embedded following the procedures outlined by us in Perez-Polo et al., 2013 (See Appendix). The antibodies used are 1:5000 Anti-NeuN (mouse monoclonal, Millipore);1:1000 Anti-myelin basic protein (mouse monoclonal, Covance); 1:1,000 Anti-IBA-1 (rabbit polyclonal, Wako); 1:250 Rat immunoglobin (IgG; Invitrogen); 1:500 anti-TauP (pSer202/Thr205; monoclonal; Thermo).

We defined mBBI using righting reflex response times (RRRT) as a criteria. Whereas sham-treated animals exhibited RRRT values of 1 to 3 minutes, mBBI animals exhibited RRRT values greater than 4 minutes.

Figure 8. RRRT Values for mBBI

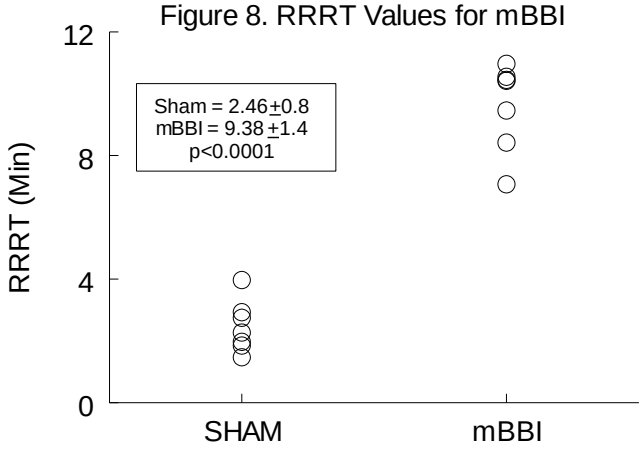

We then measured levels of the different cytokines and chemokines in hippocampus and cortex and showed comparable levels of increased IL-1α/β in animals exposed to mBBI six hours after injury using protocols described by us in Perez-Polo et al., 2013 (See Appendix) and correlated the cytokine increases with the righting reflex time responses of individual animals for different brain regions (**Figures 9-10**). There were significant increases in IL-1β and TNF-α; IL-10 also showed significant increases (data not shown, see annual report for details), consistent with our observations using the mLFP injury model. In all instances for mBBI, the hippocampus was the brain structure most consistently affected, albeit there were also significant increases in thalamus for IL-1β but not TNF-α. There was a trend to higher IL-1β and

TNF-α levels after mBBI in cortex but these were not significant due to the high inter-animal variability (**Figure 9**).

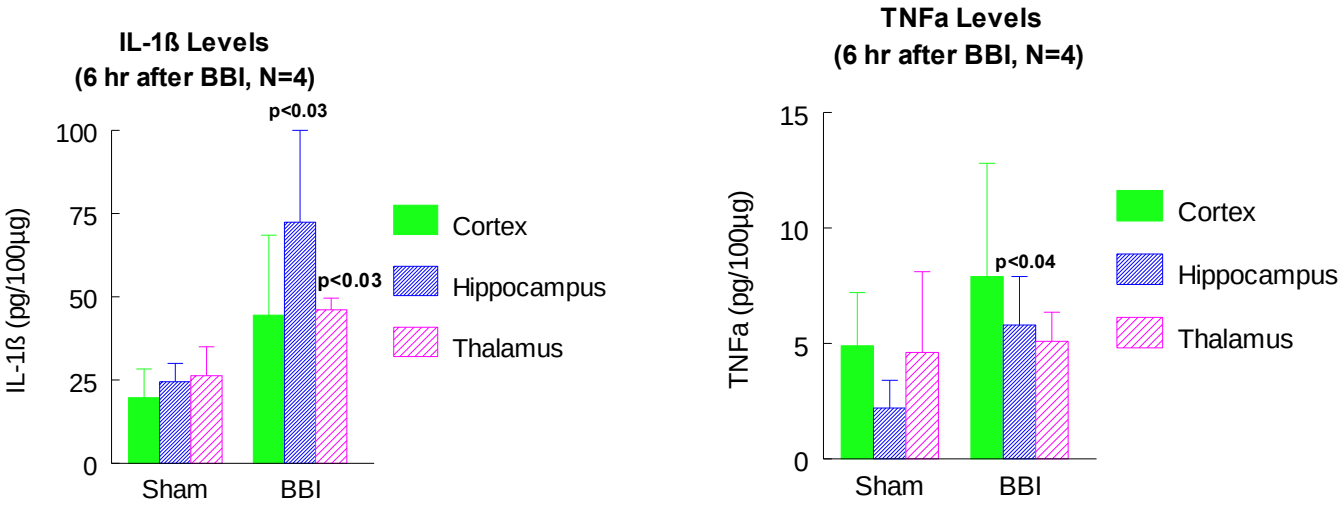

Figure 9. Cytokine protein levels in different brain regions after mBBI.

When we measured the righting reflex time after injury, a useful parameter that best mimics "return to consciousness" after TBI, preliminary analyses of the correlation between RRRT and cytokine levels showed the most consistent correlation when the hippocampus and cortex were examined (**Figure 10**). All sham values RRRT were in the 2-3.5 min range and are not shown as sham animal cytokine levels were below the level of detection. These preliminary results are consistent with our exclusionary use of RRRT in our classification of mTBI.

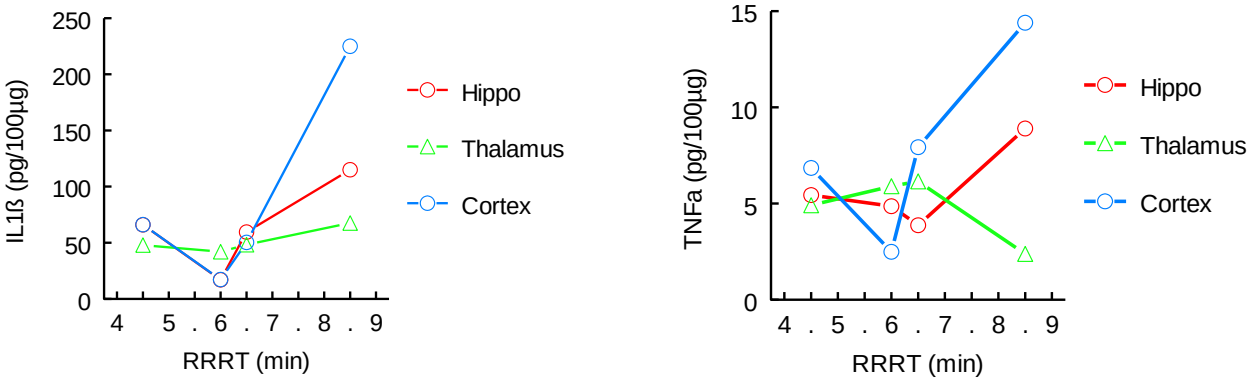

Figure 10. Correlation between cytokine levels and righting reflex response times (RRRT).

We performed preliminary qualitative assessments of the extent of incipient mBBI-induced encephalopathy relying on an immunohistological assessment of levels of p-Tau, which has been shown to correlate to the appearance of encephalopathy after TBI (McKee et al., 2009). We also observed significant increases in phosphorylated Tau protein (**p-Tau**) and the inflammatory marker associated with activated microglia and macrophages, **IBA1,** as early as 6 hours after mBBI in cortex, hippocampus, thalamus and amygdala (**Figure 11**). These results are consistent with significant inflammatory responses in cortex, hippocampus, thalamus, and amygdala six hours after mBBI. These mBBI-induced increases persisted for at least 30 days post injury. Interestingly examination of the presence of a correlation between RRRT and p-Tau or IBA-1 showed the appearance of a correlation between hippocampal p-Tau values and RRRT for hippocampus and cortex but not thalamus and amygdala (**Figure 12**). This is consistent with clinical observations of p-Tau in deceased patients suffering from TBI-induced encephalopathy. Attempts to draw a similar correlation to RRRT and IBA-1 would suggest that, opposite to the mBBI-induced increases in p-Tau, which are more brain region specific, mBBI-induced increases in IBA1 marker for inflammatory response is more widespread (**Figure 12**), a finding that is not too surprising. What we do find interesting is that the IBA1 response appears to be responsive to a threshold value of RRRT (**Figure 12).**

Figure 11. p-Tau and IBA-1 protein levels in different brain regions after BBI at 6hr and 30 days

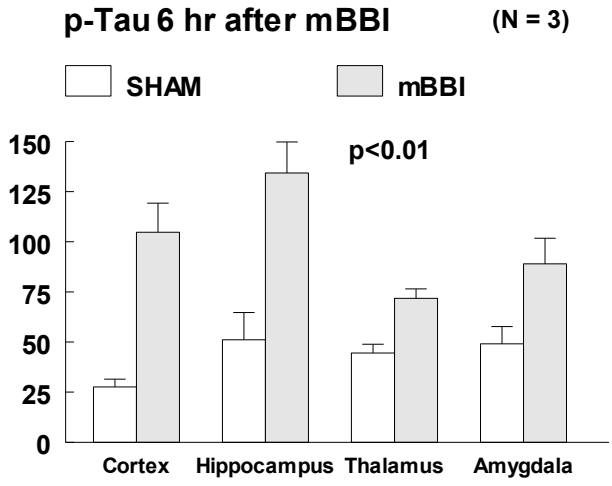

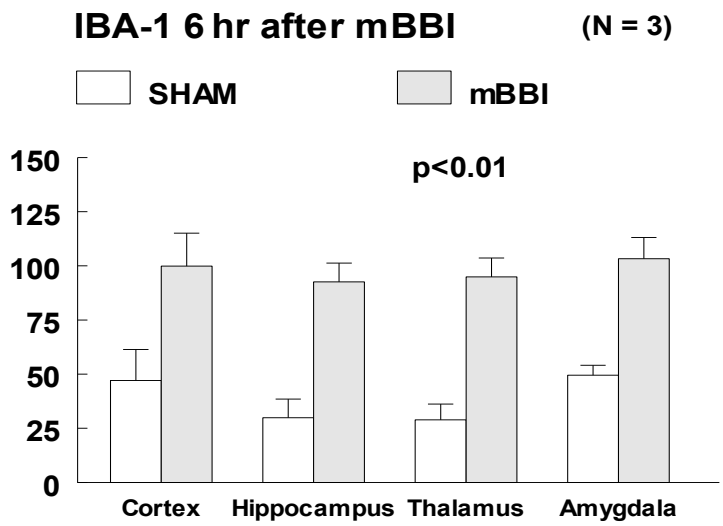

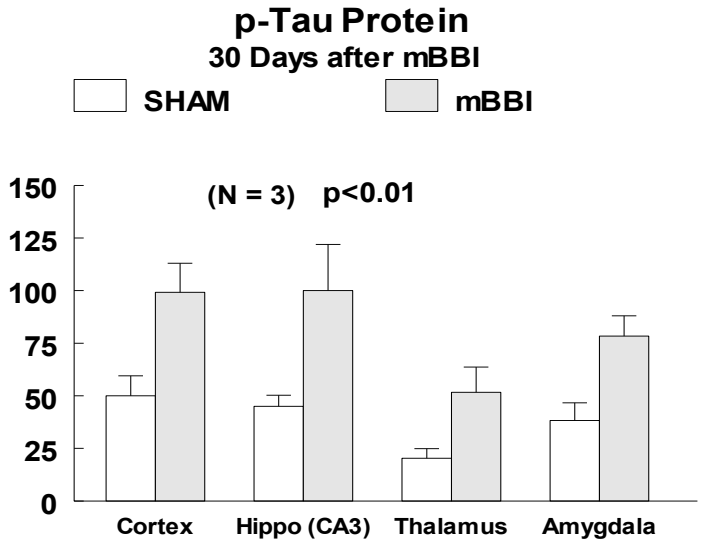

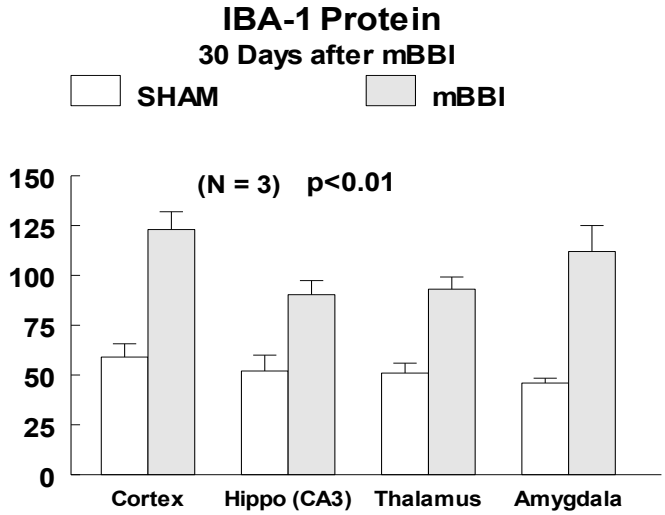

Figure 12. Correlations of p-Tau and IBA-1 protein with RRRT

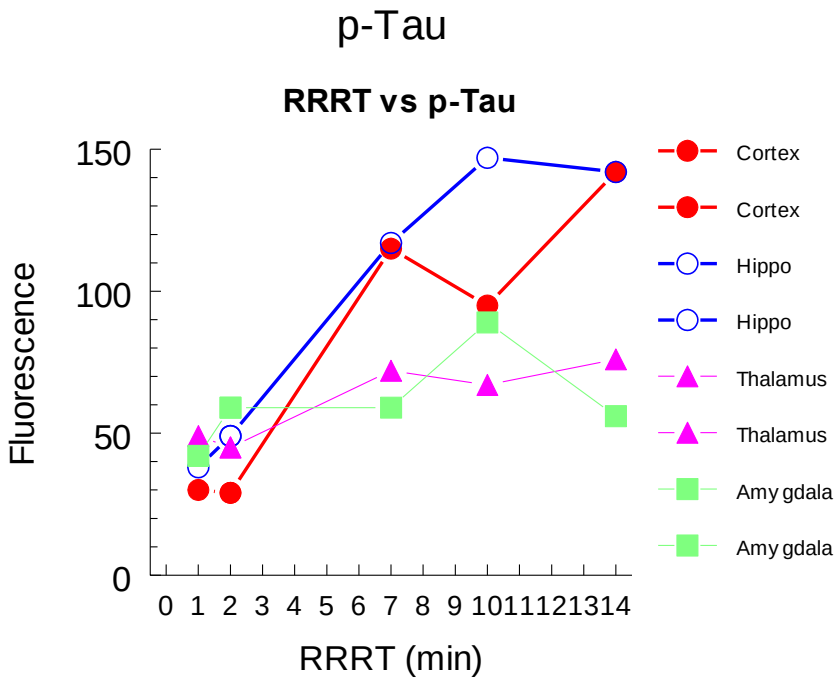

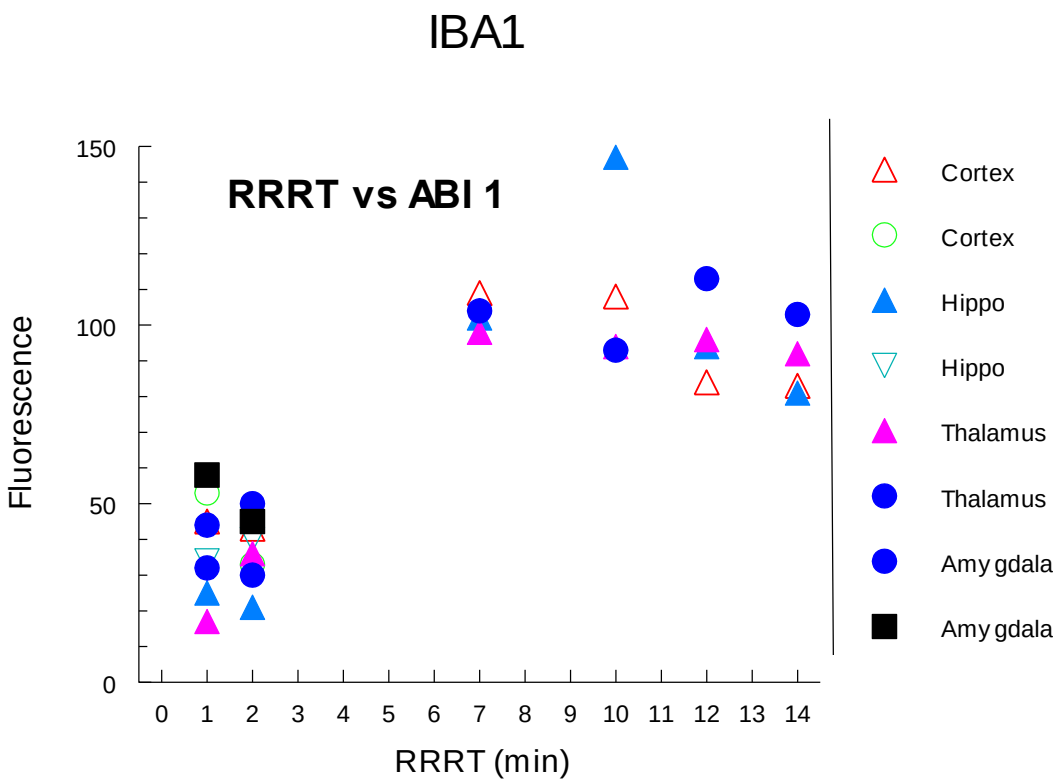

Finally, we were able to demonstrate behavioral and cognitive impairments in rats exposed to mBBI, which also appear to correlate with their individual RRR times (**Figure 13).** We find it interesting that while there was a correlation between RRRT and behavior impairments, when measured 5 days after the mBBI, there was no such correlation by day 23 after mBBI (data not shown, see annual report for details). There could be two reasons for this: (1) by day 23 brain plasticity events are compensating for the mBBI-induced dysfunction or (2) different brain regions have taken over the affected functions. Again, we lack the power to make a distinction.

Figure 13. Correlation between RRRT and time spent searching for platform

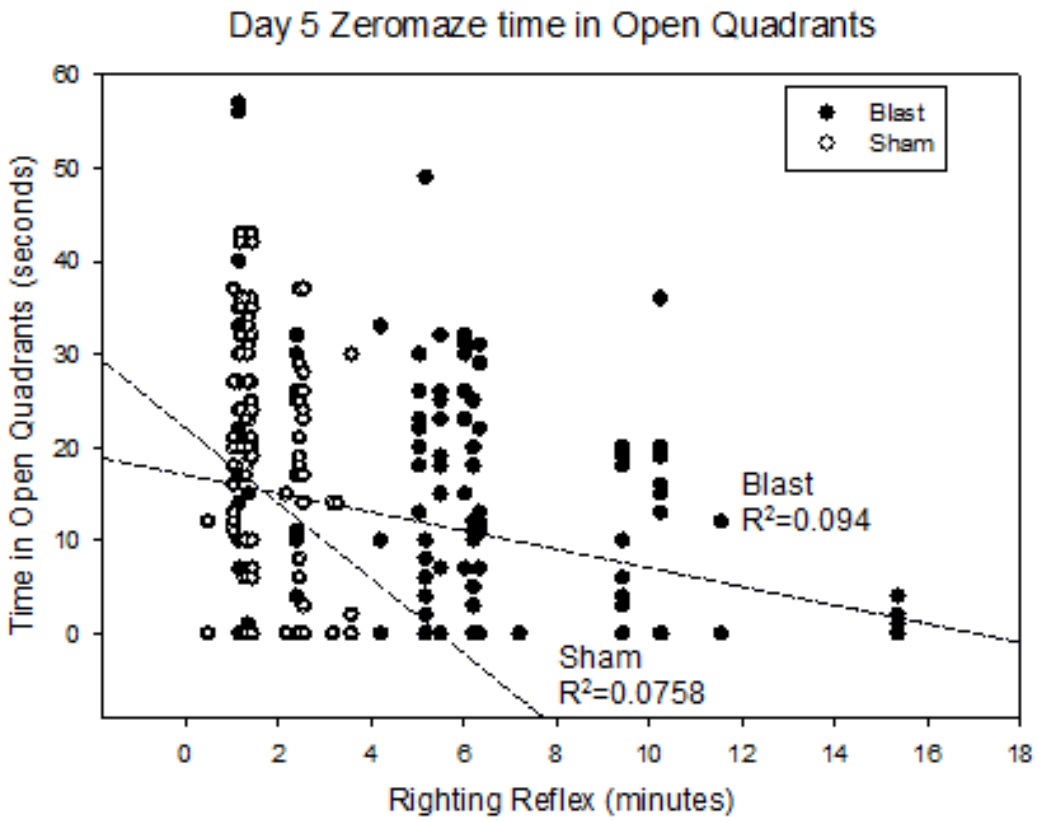

Taken together, these results would confirm the value of using the RRT time as a measure of severity of insult and likely resultant neuropathology and psychomotor/behavioral/cognitive impairment to mTBI and more specifically based on our data to date mBBI. They also present substantive evidence in favor of the hypothesis that mBBI is a high risk factor for the development of encephalopathy over time given the increased presence of p-Tau as early as six hours after injury.

Lastly, our data to date on mBBI would suggest that aside from simple inflammatory responses, there may be other mechanisms responsible for the extent of encephalopathy in common with those present in age-related neurodegenerative disease. While there is a lack of direct clinical demonstrations of

encephalopathy in mBBI perhaps eventual autopsy studies of VA patients with a clinical history of mBBI may determine the clinical importance of the observations we made in a rat model of mBBI.

Key Research Accomplishments

- We demonstrated that mTBI using two models of injury, mLFP and mBBI, stimulate the inflammatory cytokines IL-1 and TNFα
- We characterized inflammatory responses in mLFP impacting neuronal and glial losses and blood brain barrier function
- We showed that single treatments blocking the cytokine IL-1 and TNFα receptors within 6 hours of the injury ameliorate the mLFP-induced neuropathology and behavioral deficits
- We demonstrated that measuring RRRT values provides good criteria for defining mTBI
- We determined the effect of mBBI on markers for neuroencephalopathy and inflammation

Reportable Outcomes

Perez-polo et al, 2013 see Appendix

Conclusion

Blocking the cytokine IL-1 and TNFα receptors with FDA-approved drugs can ameliorate mTBI outcomes in the rat.

Mild brain blast injury in the rat results in significant increases in established neuroencephalopathy and inflammation markers

Preclinical studies of these two drug treatments are necessary given their potential for therapeutic use

References

Cantu, R.C., Chronic traumatic encephalopathy in the National Football League, Neurosurgery 61:223–225, 2007

Dixon CE, Lyeth BG, Povlishock JT, Findling RL, Hamm RJ, Marmarou A, Young HF, and Hayes RL. (1987) A fluid percussion model of experimental brain injury in the rat. J Neurosurg. 67, 110-9.

Donkin JJ. Nimmo AJ. Cernak I. Blumbergs PC. Vink R. Substance p is associated with the development of brain edema and functional deficits after traumatic brain injury. J Cereb Blood Flow Metab 29: 1388-1398, 2009.

Elder GA, Dorr NP, DeGasperi R, Sosa MAG, Shangness MC, Maudlin-Guonimo E, Hall AA, McCarron RM, Ahlers ST, (2012) J. Neurotrauma 29:2564-2575.

Hogue CW, McGurk D, Thomas JL, Cox AL, Engel CC, Castro CA, (2008) Mild traumatic brain injury in U.S. soldiers returning from Iraq. N. Engl. J. Med. 358:453-463.

Israelson, C., Bengsston, H., Kylberg, A., Kullander, K., Lewen, A., Hillered, L., Ebendal, T. (2008) Distinct Cellular Patterns of Upregulated Chemokine Expression Supporting a Prominent Inflammatory Role in Traumatic Brain Injury. J. Neurotrauma. 25: 959-974.

Kamnash A, Kwon S-K, Kovesdi E, Ahmed F, Barry E, Grundberg NE, Long J, Agoston D (2012) Electrophoresis 33:3680-3692.

Levin HS, Wilde E, Troyanskaya M, Petersen NJ, Scheibel R, Newsome M, Radaideh M, Wu T, YallanPalli R, Chu Z, Li X. (2010) J. Neurotrauma 27:683-694.

McKee AC, Cantu RC, Nowinski CJ, Hedley-Whyte ET, Gavett BE, Budson AE, Santini VE, Lee H-S, Kubilus CA, Stern RA.(2009) Chronic traumatic encephalopathy in athletes: progressive tauopathy after repetitive head injury. J. Neuropath. Exp. Neurol, 68:709-35.

Omalu, B.I,, DeKosky, S. T., Hamilton, R. L.,Minster, R. L., Kamboh, M. I., Shakir, A. M., & Wecht, C. H. (2006). Chronic traumatic encephalopathy in a national football league player: Part II. Neurosurgery, 59(5), 1086–1092

Perez-Polo JR. Rea HC. Johnson KM. Parsley MA. Unabia GC. Xu G. Infante SK. Dewitt DS. Hulsebosch CE. (20130 Inflammatory consequences in a rodent model of mild traumatic brain injury. J. Neurotrauma. 30:727-40.

Appendices

JOURNAL OF NEUROTRAUMA 30:727–740 (May 1, 2013)

DOI: 10.1089/neu.2012.2650

Inflammatory Consequences in a Rodent Model of Mild Traumatic Brain Injury

J. Regino Perez-Polo,[1] Harriet C. Rea,[1] Kathia M. Johnson,[1] Margaret A. Parsley,[1,2] Geda C. Unabia,[1] GuoJing Xu,[1] Smitha K. Infante,[1] Douglas S. DeWitt,[2] and Claire E. Hulsebosch[3]

Abstract

Mild traumatic brain injury (mTBI), particularly mild ''blast type'' injuries resulting from improvised exploding devices and many sport-caused injuries to the brain, result in long-term impairment of cognition and behavior. Our central hypothesis is that there are inflammatory consequences to mTBI that persist over time and, in part, are responsible for resultant pathogenesis and clinical outcomes. We used an adaptation (1 atmosphere pressure) of a well-characterized moderate-to-severe brain lateral fluid percussion (LFP) brain injury rat model. Our mild LFP injury resulted in acute increases in interleukin-1α/β and tumor necrosis factor alpha levels, macrophage/microglial and astrocytic activation, evidence of heightened cellular stress, and blood–brain barrier (BBB) dysfunction that were evident as early as 3-6 h postinjury. Both glial activation and BBB dysfunction persisted for 18 days postinjury.

Key words: astrocytes; blood–brain barrier; cytokines; inflammation; mild traumatic brain injury

Introduction

Moderate-to-severe traumatic brain injury (TBI) is known to trigger inflammatory pathways, in part, by increases in cytokines and chemokines that result in monocyte cellular activation and infiltration, glial activation, neuronal and myelin loss, and further persistent inflammation.[1,2] For example, interleukin (IL)-1α/β and tumor necrosis factor alpha (TNF-α) have been shown to increase transiently after moderate-to-severe TBI with the accompanying development of pathology.[3–7] Injury-induced increases in IL-1α/β and TNF-α in the central nervous system (CNS) have been shown to be prompt and robust, typically peaking within 3–6 h postinjury.[8–16]

Although there is an ample body of literature on the role of brain ischemia, excitotoxicity, oxidative stress (OS), inflammation, and edema in moderate-to-severe TBI, less is known about its mild counterpart.[17–21] Early events triggered by TBI include increases in the cytokines, IL-1β and TNF-α, known to contribute to monocyte cellular activation and infiltration, glial activation, neuronal and myelin loss, and further persistent inflammation.[1–7]

Mild traumatic brain injury (mTBI), particularly mild ''blast type'' injuries resulting from improvised exploding devices and many sport-caused injuries to the brain, result in long-term impairment of cognition and behavior.[22–25] Our central hypothesis is that increases in IL-1α/β and TNF-α levels after mTBI may be responsible, in part, for triggering a cascade of inflammation with downstream effects on glial activation, neuronal function impairment, and blood–brain barrier (BBB) integrity. Behavioral and cognitive impairments are demonstrable for several rodent models of TBI by day 15 postinjury.[26–28] Thus, we performed our assessments of inflammatory macrophage and microglial activation and BBB dysfunction at 3 and 6 h and 18 days postinjury. A corollary to our hypothesis is that the inflammatory consequences of mild lateral fluid percussion (mLFP) injury may persist and contribute to the development of long-term brain impairments associated with mTBI.

The rat lateral fluid percussion model of TBI[29,30] is widely accepted and causes a combination of focal cortical contusion and diffuse injury of subcortical brain areas, much like that present in human brain neuropathology after TBI.[31] We adapted the LFP injury model by decreasing the effect to 1 atmosphere (atm) pressure, which resulted in righting reflex response times of more than 4 min, but less than 10 min, as compared to righting reflex response times in excess of 15–30 min characteristic of moderate-to-severe LFP injury. We characterized the mLFP injury model at 3–6 h and 18 days postinjury in terms of acute inflammation biomarkers, such as increased IL-1α/β and TNF-α, macrophage/microglial and astrocytic activation, impaired BBB function, and activating transcription factor 3 (ATF-3) transcription factor activation, all known to affect brain function.

Methods

Surgical preparation: LFP injury

All animal manipulations were approved by the Department of Defense (DoD) and the University of Texas Medical Branch

Departments of [1]Biochemistry and Molecular Biology, [2]Anesthesiology, and [3]Neuroscience and Cell Biology, University of Texas Medical Branch, Galveston, Texas.

(Galveston, TX) institutional animal care committees, using guidelines developed by the DoD and National Institutes of Health (Bethesda, MD). Initial experiments were performed with LFP brain injury on rats at 1, 2, and 2.4 atm for comparison purposes, where the 2.0- and 2.4-atm levels of injury are known to result in what have been labeled in the literature as a moderate-to-severe TBI.[29,30] We defined mLFP based on righting reflex responses in the 4–10-min range after a 1-atm injury. Thus, all the immunohistochemical (IHC) assessments were performed on rats experiencing the 1-atm mLFP injury. Briefly, male Sprague-Dawley rats, weighing 350–400 g, were anesthetized with isoflurane in an anesthetic chamber, intubated, and mechanically ventilated with 1.5–2.0% isoflurane in O_2/room air (30:70) using a volume ventilator (Edco Scientific, Inc., Chapel Hill, NC). Rats were then placed in a stereotaxic frame, and the scalp was sagittally incised. A 4.0-mm diameter hole was trephined into the skull 2.0 mm to the right of the sagittal suture and midway between the lambda and bregma. A modified Luerlok syringe hub was placed over the exposed dura, bonded in place with cyanoacrylic adhesive, and covered with dental acrylic. Isoflurane was discontinued; rats were connected to the trauma device and subjected to a mild 1.0-atm fluid-percussion injury, immediately after acquisition of a withdrawal reflex to paw pinch. The sham group was treated as described above, with the exception that no fluid-percussion injury was administered. After mLFP or sham injury, rats were disconnected from the fluid percussion device and righting reflex was assessed every 60 sec until there was a normal righting reflex. To test righting reflex, rats were placed on their backs and the time at which the animal righted itself 3 times consecutively was recorded as the righting reflex. Rats were then placed on 2% isoflurane, and wound sites were infused with bupivicaine and sutured with prolene. Isoflurane was discontinued, and rats were extubated and allowed to recover in a warm, humidified incubator.

Rats were allowed to recover for 3- or 6-h survival periods or 18 days, at which time rats were anesthetized before sacrifice with 150 mg/kg of Nembutal intraperitoneally and perfused transcardially with 4% paraformaldehyde (PFA) for IHC or, if earmarked for immunoassays, they were sacrificed and the hippocampus, parietal cortex, and thalamus were dissected and stored at −80°C until use.

Perfused brains were removed, postfixed overnight in 4% PFA, blocked into 3–4-mm coronal sections, and transferred to 30% sucrose until penetration was complete. Tissue was then embedded in optimal cutting temperature compound and frozen at −20°C. Tissue was mounted and then sectioned at 30 or 50 μm and collected both serially and free-floating. Once sectioned, every ninth section was collected for assessment with hematoxylin and eosin staining to provide a gross indicator of lesion severity. Sections were processed for widefield epifluorescent and confocal visualization as follows: A series of sections (every ninth section from the rostral to caudal extent) were rinsed in Tris-buffered saline (TBS), followed by incubation in TBS plus 0.025% Triton X-100 plus 5% serum of the appropriate species for 1 or 2 h. Parafin-embedded 3-mm-thick coronal blocks were sectioned at 5 um on a rotary microtome and immediately placed in dH_2O at 46°C and placed on slides. Sections were deparaffinized at 56°C and rehydrated with xylene and a series of ethanols (100%, 95%, and 80%), followed by dH_2O and phosphate-buffered saline (PBS). After the antigen retrieval step with 10 mM of Na citrate (pH 6.0 at 100°C for 30 min), tissue was washed in 0.18 M of PBS 4 times, blocked with 5% normal goat serum (NGS) plus 0.3% bovine serum albumin (BSA) in 0.18 M of PBS for 30 min. Sections were incubated with an antibody (Ab) in 1% NGS plus 0.3% BSA/0.025% Triton X-100 for 2 h at room temperature (RT), followed by washing 3 times with PBS plus Triton X-100 for 10 min, each at RT.

Except for sections incubated in secondary Ab in the absence of a primary Ab (negative control), sections were incubated in primary Ab or Abs for multi-antigen visualization overnight at 4°C on a rotating platform. Sections were then rinsed thrice in TBS and incubated in the appropriate secondary linked to an Alexa Fluor® dye (Molecular Probes, Eugene, OR) that excites at either 488 (green) or 568 (red) nm for 3 h. Sections were then mounted onto glass cover-slips, allowed to briefly dry, then mounted to glass slides using Fluoromount-G, after which slides were allowed to sit at RT for at least 20 min and were then put in a refrigerator for at least 24 h before storage in a freezer until viewing. For wide-field epifluorescent assessment and image acquisition, slides were viewed on an upright microscope with narrow band-pass filters to minimize fluorescence overlap and images were captured using a SPOT Flex digital camera (Diagnostic Instruments, Inc., Sterling Heights, MI) before annotation using Adobe Photoshop CS4. For confocal acquisition, slides were first visualized under wide-field epifluorescent light on an Olympus BX51 upright microscope (Olympus, Tokyo, Japan). Suitable fields were imaged using a Bio-Rad Radiance 2000 confocal system (Bio-Rad, Hercules, CA). Resulting images represent projections from stacks of optical sections of no less than 25 and no greater than 30.

Abs used were as follows 1:20 IL-1β (goat polyclonal; R&D Systems, Minneapolis, MN); 1:5000 anti-NeuN (mouse monoclonal; Millipore, Billerica, MA);1:1000 anti-myelin basic protein (mouse monoclonal; Covance Inc., Princeton, NJ); 1:200 anti-RECA-1 (rat endothelium cell antigen 1; mouse monoclonal; AbD Serotec, Oxford, UK); 1:1000 anti-IBA-1 (ionized calcium-binding adapter molecule 1; rabbit polyclonal; Wako, Richmond, VA); 1:1000 anti-GFAP (glial fibrillary acidic protein; rabbit polyoclonal; Dako, Glostrup, Denmark); 1:1000 anti-GFAP (mouse monoclonal; Chemicon International, Temecula, CA); 1:400 anti-vimentin (mouse monoclonal; Sigma-Aldrich, St. Louis, MO); 1:1000 anti-nestin (chicken polyclonal; Millipore); 1:750 albumin (ALB; sheep polyclonal; Bethyl Laboratories, Inc., Montgomery, TX); 1:250 rat immunoglobulin G (IgG; Invitrogen, Carlsbad, CA); 1:20 IL-1β (goat polyclonal; R&D Systems), 1:1000 anti ATF-3 (rabbit polyclonal; Santa Cruz Biotechnology, Santa Cruz, CA); and 1:3000 anti-SMI 71 (mouse monoclonal; Covance).

We incubated sections with 1:1000 Alexa Fluor 568 (red) or 488 (green) goat anti-rabbit IgG or goat anti-mouse IgG for 2 h at RT (shaking). We mounted sections on slides, dried for a few minutes, and added regular mounting medium and let slides sit at RT for at least 20 min, after which they were put in a refrigerator for at least 24 h before storage in a freezer until viewing.

Cytokine immunoassay

We measured cytokines using the Bio-Plex assay kit from Bio-Rad, a capture sandwich immunoassay that is very sensitive at detecting cytokines in the pg/mL range.

The Bio-Plex cytokine assay is a multi-plex bead-based assay designed to detect up to 100 cytokines in a single well of a 96-well plate. The assay uses up to 100 color-coded bead sets, which are conjugated with different specific reactants. Each reactant is specific for a different target molecule. Specific reaction is identified based on bead color. Samples in each well are drawn up into the flow-based Bio-Plex array reader. The reaction is measured by using fluorescently labeled reporter molecules that are also specific for each target protein. For our experiment, the Bio-Plex rat cytokine/chemokine assay was designed to detect and quantitate nine rat cytokines/chemokines: IL-1α; IL-1β; TNF-α; IL-2; IL-6; IL-4; IL-10; granulocyte macrophage colony-stimulating factor (GM-CSF), and interferon-gamma.

Image capture

Confocal images were acquired from immunofluorescently (IF) serial-labeled serial sections 40 um thick from at least three

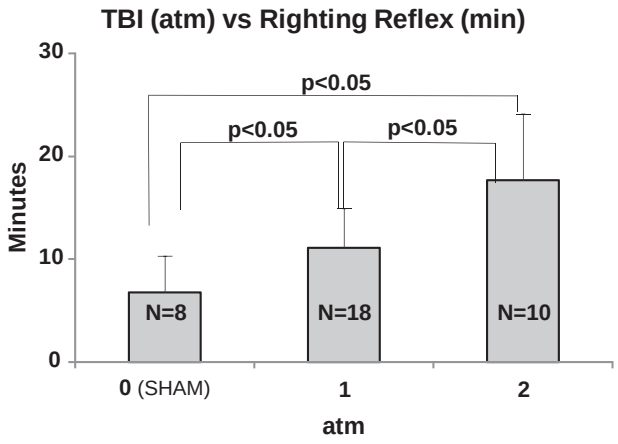

FIG. 1. Time of righting reflex responses in minutes as a function of mLFP injury severity measured in atm. Responses for 1 and 2 atm mLFP injuries are significantly different from shams (0 atmospheres) and from each other ($p < 0.05$).

sections per animal, for 3 different animals for further sequential analysis. Each sample was initially compared by observing z-stack, optical selections 10 um thick, to verify planar continuity of sections. Conditions for scanning were 20× lens, no zoom, and an acquisition resolution of 1280×1024 pixels. Fixed iris (pinhole), laser intensity,

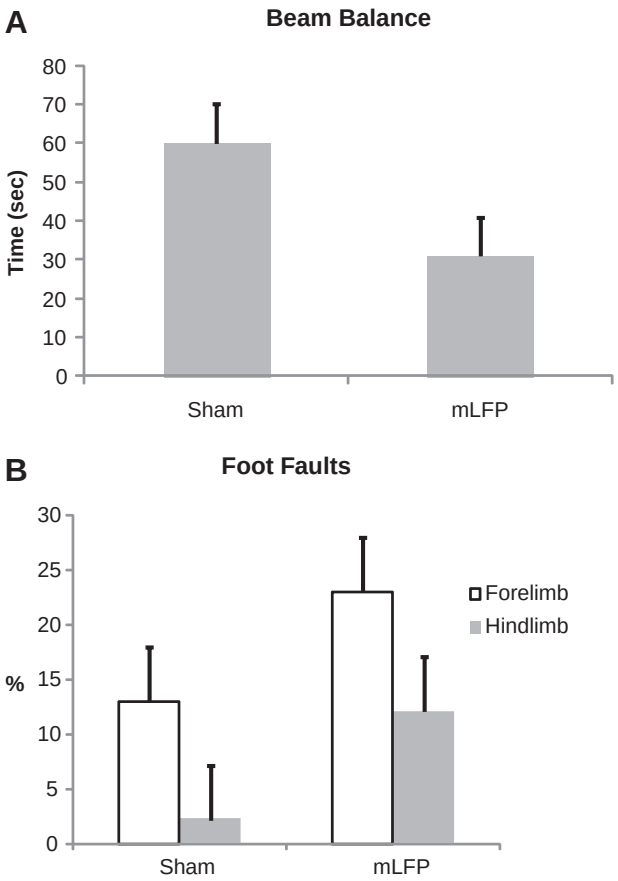

FIG. 2. **(A)** Beam balance duration for rats 11 days after 1-atm mLFP injury ($p < 0.05$, compared to shams). **(B)** Forelimb and hindlimb foot faults 11 days after 1-atm mLFP injury ($p < 0.05$, compared to shams).

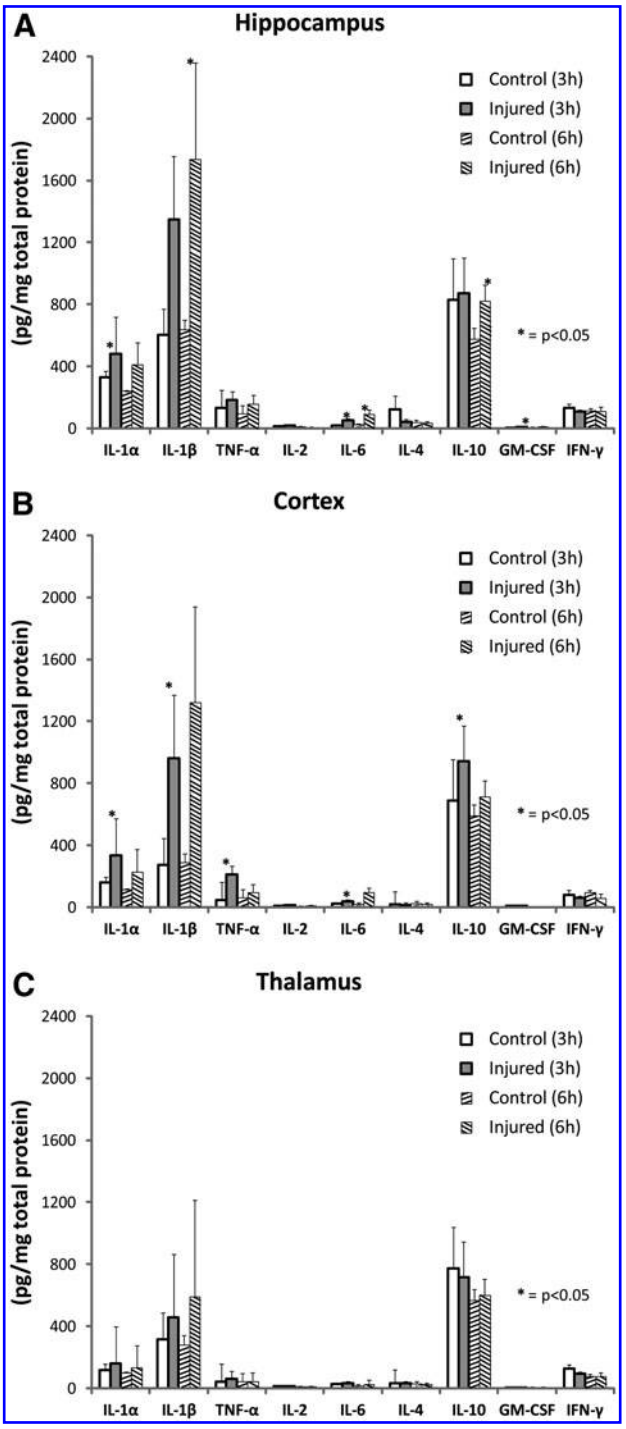

FIG. 3. **(A)** Hippocampal, **(B)** parietal cortical, and **(C)** thalamic cytokine protein levels at 3 and 6 h after 1-atm mLFP injury. Significant differences between injured (ipsilateral) and control (contralateral) values are $p < 0.05$. **(D)** Representative image of IL-1 β near site of injury 18 days after mLFP injury (original magnification, scale bar = 100 microns). Color image is available online at www.liebertpub.com/neu

gain, and offset were maintained throughout all samples of the same experiment. Images were taken at the same optical thickness (2 or 5 um) for all groups, based on countable cell numbers of biomarker-stained proteins present. Images on paraffin-embedded IHC sections 5 um thick, probed for endothelial barrier antigen (EBA)

FIG. 3. (Continued).

expression, were photographed by light microscopy at 20×. Counts were tallied and compared from unlabeled printed images taken on ipsilateral and contralateral sides of the same section.

Cell/intensity quantitation

Cell profiles for various markers were counted in specific anatomic regions (e.g., hippocampus CA1, dendate gyrus, and so forth) on histolgical sections, from at least three sections per animal, for at least 3 different animals, averaged, and calculated as means of profile counts ± standard deviation within that specific region/animal/brain hemisphere. Thus, the final number was a mean number of profiles counted within a three-dimensional region (area of anatomical region × thickness of section). Thicknesses of sections were not significantly different between the ipsilateral and contralateral side for any given section; cell counts were stereological estimates based on profile counts. For each section, counts were performed by three different individuals on a blinded basis to eliminate bias. Though there were differences in resulting counts for any slice for the three different individuals counting, the relative differences between samples were consistent and there was a 10% or less variation for any sample count across individual counts from the three individuals performing counts.

For some analyses, it was not possible to count cell profiles (e.g., Iba-1, GFAP, and so forth). For these comparisons, after ensuring that staining was linearly related to secondary reporters, density of immunoreaction product was quantified utilizing optometric techniques. Analysis was performed using a Bio-Rad confocal laser system coupled to a Nikon light microscope using Bio-Rad 1.50 software. Sections ($n = 5$/animal) from each group at each time point were viewed with a 10× objective, and images were captured using a SPOT Megapixel camera. The final projected image for analysis was 1000× that of the original section for cytological analyses. Thus, pixels were included in the analysis that were not readily detectable in the low-magnification photodocumentation shown in the results. Integrated optical density area was confined and measured in the regions listed above. Density levels and distribution were quantified both ipsilaterally and contralaterally and compared to data collected from shams. For all sections, nonstaining gray or white matter was empirically chosen as background and staining was normalized to this signal intensity.

Beam balance assay

At day 11 postinjury or post–sham treatment, rats were placed on a balance beam apparatus consisting of a beam 91.5 cm long (L) × 1.7 cm wide (W) elevated 30 cm off the surface below and secured to a platform on either end. Rats were placed on the center of the beam and released (start time) and were allowed to walk to either end. Animals were returned to the center of the platform if they walked onto one of the end platforms. This was continued for 1 min or until rats fell off (stop time). For each rat, 10 trials were performed and average time duration on the beam was recorded. Naïve rats were also tested for purposes of establishing a baseline.

Foot fault assay

At day 11 postinjury or post–sham treatment, rats were placed on a wire mesh 69.5 cm W × 45 cm L with 3-cm gaps stretched out over a wooded frame. The number of times from 10 attempts on the wire mesh that the forelimb or hindlimb fell through the gaps rats transversed the mesh were recorded separately as a percentage (% foot faults).

Statistical analyses

Analyses were performed with GraphPad Prism 5 software (GraphPad Software, San Diego, CA). For analyses involving two groups, a Student's *t*-test was performed and a *p*-value less than 0.05 was considered significant. If variances for two groups were deemed significantly different, a Welsh correction was added to the Student's *t*-test. For analyses of more than two groups, a one-way analysis of variance was performed with a Tukey-Kramer post-hoc test to compare groups. A *p*-value less than 0.05 was deemed significant.

Results

There were increased righting reflex response times for rats after mLFP injury

An accepted measure of the severity of a TBI incident in humans is the return of consciousness, which, in rodent models, is mimicked by measuring the righting reflex response time. In our LFP injury model, we observed a significant increase in righting reflex response times of approximately 75% after injury with a 1-atm LFP injury. Righting reflex response time after LFP increased as the impact force was increased to 2 atm, the latter being typically used in moderate-to-severe LFP injury models (Fig. 1). All subsequent experiments were performed using the 1-atm LFP injury as a model of mLFP with righting reflex response times greater than 4 min or lesser than 10 min.

Locomotor responses to mLFP injury after 11 days of show impaired function

One index of injurious outcome often used in assessments of TBI in rodent models is the measurement of vestibulomotor function, as assessed by measuring the time that a rat can balance on a beam

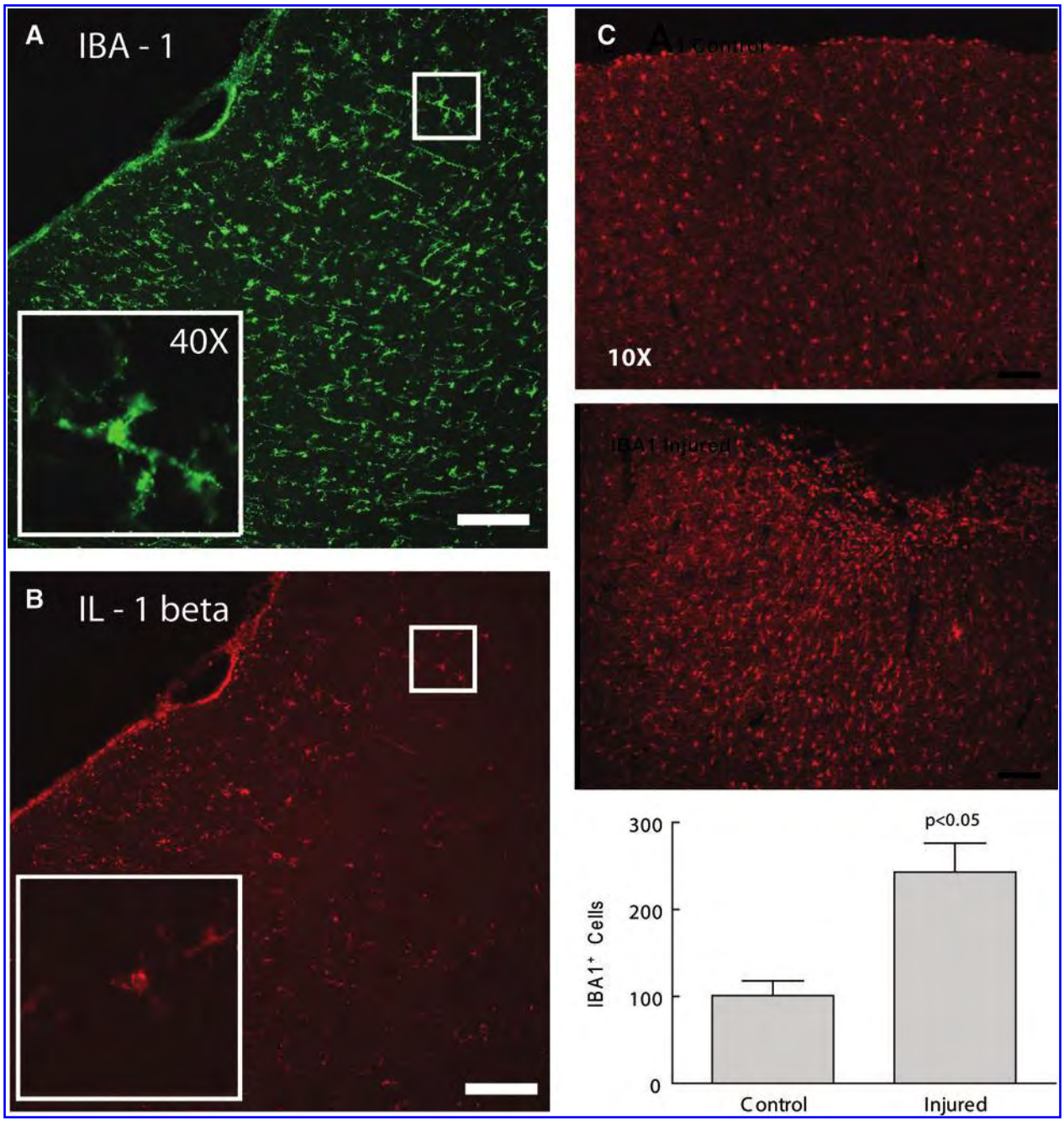

FIG. 4. Representative images of cortical inflammatory response. **(A)** IBA-1 green and **(B)** IL-1β red immunostatining 6 h after 1-atm mLFP injury at site of injury (original magnification, 10×). Insets display ''reactive'' morphological phenotype (original magnification, 40×). **(C)** IBA-1 cortical immunostatining 18 days after 1-atm mLFP injury near injury site (original magnification, 10×). Quantitation of cortical IBA-1^+ cells 18 days after mLFP injury ($p < 0.05$) (scale bars = 100 microns). Color image is available online at www.liebertpub.com/neu

with defined dimensions[32] and the number of foot faults incurred by a rat transversing a mesh with specific parameters.[33] Exposure to mLFP injury showed a significant impairment in both balance ability and locomotor coordination at 11 days postinjury (Fig. 2).

mLFP increases cytokine expression at 3–6 h

We focused on early time points after injury given the known prompt and robust inflammatory response to the more moderate and severe brain injury reported for rat TBI models, spinal cord injury, and ischemia.[13–15] Injury to the brain is known to have an early component in which prompt cell-death–promoting signaling mechanisms are triggered, followed by the prompt activation of signaling pathways responsible for more-pervasive delayed chronic inflammation and persistent plastic changes. Thus, we chose the 3- and 6-h time points as useful for acute biomarker-based assessments to characterize this mild version of brain injury.

To test the hypothesis that mLFP injury triggers an early inflammatory response, we compared ipsilateral (right hemisphere, injured) to contralateral levels of nine cytokines in three brain

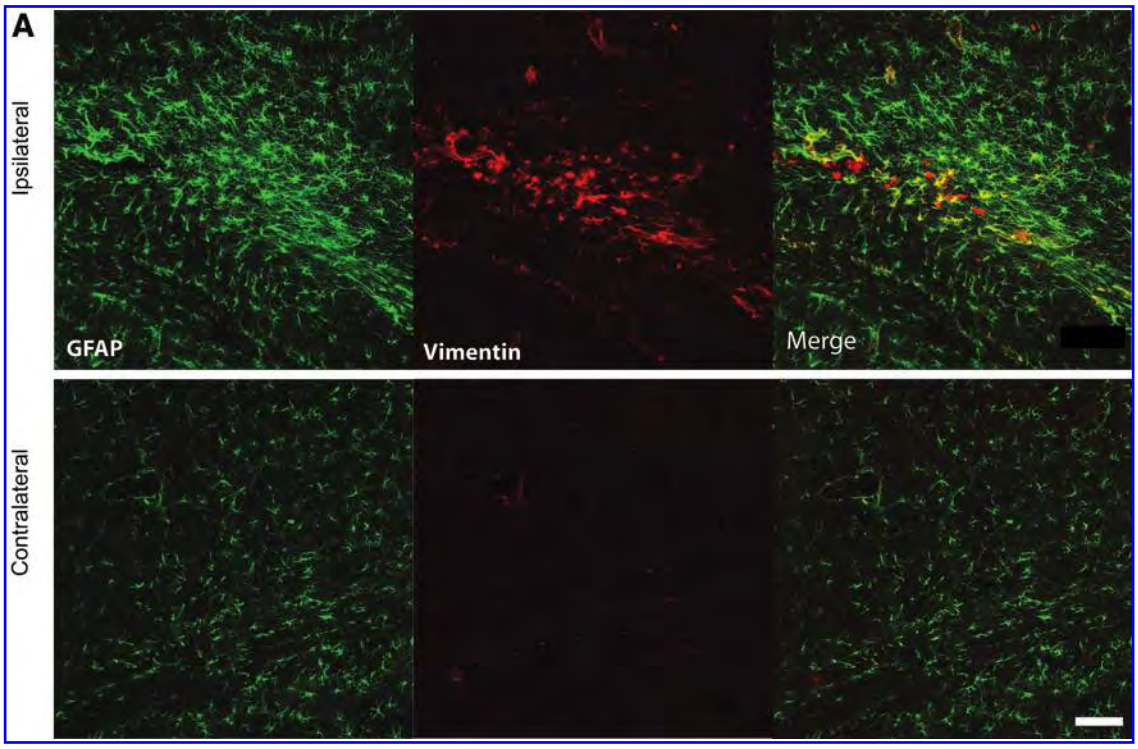

FIG. 5. Representative immunostaining 6 h after 1-atm mLFP injury. Images of inflammatory activated astrocytes in ipsilateral parietal corticex, as indicated by GFAP$^+$ cells and colocalized **(A)** vimentin (scale bar = 50 microns). **(B)** Cortical astrocytic activation 18 days after mLFP injury, as indicated by GFAP immunostaining (original magnification, 20×). Quantitation of cortical GFAP$^+$ cells 18 days after mLFP injury ($p < 0.05$). Color image is available online at www.liebertpub.com/neu

regions (parietal cortex, hippocampus, and thalamus), using an array immunoassay that measures cytokines in the pg/g cytokine protein/total protein range (Fig. 3A–C). In the ipsilateral parietal cortices, compared to their contralateral counterparts, there were significant increases in levels of IL-1α, IL-1β, and TNF-α as early as 3 h after mLFP injury. By 6 h, there were also significant increases in IL-1α, IL-1β, TNF-α, IL-6, and IL-10 (a noninflammatory cytokine) as well. Increases in IL-1β were the most prominent, relative to changes in all the other inflammatory cytokines. In the ipsilateral injured hippocampi, there were significant increases in levels of IL-1α, IL-1β, TNF-α, and IL-6 as early as 3 h after mLFP injury, when comparing ipsilateral to contralateral hemispheres. By 6 h, there were also significant increases in IL-1α, IL-1β, TNF-α, IL-6, and the anti-inflammatory IL-10 as well. Again, increases in IL-1β were the most prominent, relative to the changes in all the other cytokines. In the ipsilateral injured thalami, ony IL-1β showed significant increases at 6 h after mLFP injury, when comparing ipsilateral to contralateral hemispheres. By 18 days postinjury, we could only detect, by IHC for IL-1β, its presence in a sparse population of IL-1β^+ cells proximal to the site of injury (Fig. 3B).

mLFP injury increases the levels of inflammatory cellular markers after 3–6 h

Increases in parenchymal levels of IBA-1 are associated with an increased presence of activated macrophages and microglia, both indicators of an ongoing inflammatory response. Six hours after mLFP injury, there was a significant increase in IBA-1$^+$ cells throughout the cortex, which colocalized with IL-1β and displayed a ''reactive'' morphological phenotype (Fig. 4), consistent with inflammation. This increased localized IBA-1 presence persisted for 18 days after injury (Fig. 4C).

mLFP increases astrocytic activation

Given the increased levels of inflammatory cytokines and the increase in levels of the inflammatory marker, IBA-1, as early as 3–6 h after mLFP injury, we used IF to assess the state of activation of astrocytes, also known to play a role in inflammatory responses in the CNS.[34,35] As early as 6 h after mLFP injury, there was a significant increase in GFAP staining intensity (GFAP$^+$), a marker for astrocytic activation, in the cingulate cortex ipsilateral to the injury site (Fig. 5). Figure 5 shows the classical star-like hypertrophied configuration of astrocytes responding to injury that, in part, defines the inflammatory cascade induced by CNS trauma and is a contributor to later pathology. We observed similar levels of activation in the thalamus and hippocampus (data not shown). The injury-induced increase in GFAP$^+$ cell labeling persisted for 18 days. We also used the glial biomarkers, nestin and vimentin, and, as can be seen in Figure 5, the mFLP injury induced significant increases in nestin and vimentin labeling of activated astrocytes.

mLFP perturbs the BBB

Moderate-to-severe TBI is known to cause significant perturbations in the integrity of the BBB with the resulting influx of blood-derived substances, such as ALB and IgG, contributing to a growing state of inflammation and OS.[20,36,37] It was unclear, however, whether an injury that can be described as mild would elicit a similar loss of BBB integrity and subsequent release of blood-derived proteins. We therefore asked whether there was

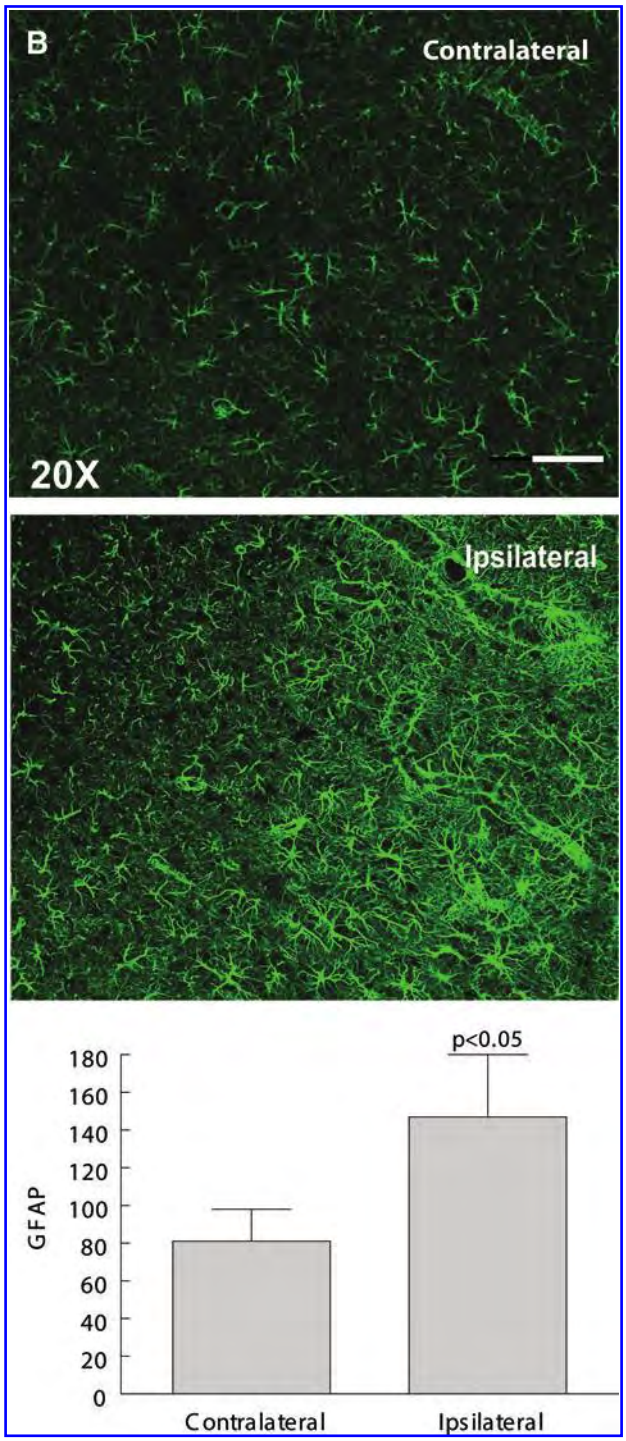

FIG. 5. (Continued).

evidence of an mLP injury-induced BBB breakdown that would allow, and perhaps stimulate, intrusion of injury-activated macrophages as well as the blood-derived proteins, ALB and IgG, into the parenchyma. Both were significantly increased at the site of injury in the parenchyma after mLFP injury, when compared to controls (Fig. 6). There was also a decreased appearance of EBA, as detected with the SMI-71 Ab, a marker for BBB integrity and more direct indicator of compromised BBB integrity (Fig. 6 A–C). These changes persisted up to 18 days after mLFP injury when they colocalized to the endothelial lining of blood vessels, as shown by colocalization with the RECA, an endothelial marker consistent with impaired BBB functionality (Fig. 6 D–E).

There was neuronal loss in the hippocampus of rats 18 days after mLFP injury

To determine the identity of the tissue loss in brains of rats exposed to mLFP injury after 18 days, cells were stained for NeuN, a marker for neuronal nuclei. Eighteen days after mLFP injury, there was significant neuronal loss of more than 50% of $NeuN^+$ cells in the ipsilateral hippocampus, as compared to sham-treated rats. Although there was also significant neuronal loss in the contralateral hippocampus, compared to shams, contralateral hippocampi also showed more severe neuronal losses, compared to their ipsilateral conuterparts (Fig. 7).

There was significant myelin loss 18 days after mLFP injury

A significant indicator of neuronal dysfunction is the extent of losses in neuronal myelination. We measured the relative loss of myelin in hippocampus by IHC using a myelin basic protein (MBP) Ab. Eighteen days after mLFP injury, we observed a better than 40% loss in MBP IF consistent with neural dysfunction (Fig. 8).

Discussion

Mild ''blast'' injuries resulting from improvised exploding devices have long-term cognitive and behavioral deficits stemming from mTBI that seriously impair quality of life. Brain damage is a result of the initial mechanical trauma (or primary inury) and delayed secondary events. Secondary events include breakdown of the BBB, edema formation with concomitant swelling, infiltration of peripherally circulating blood cells, activation of resident glial cells, and increased parenchymal levels of stress-response proteins, including proinflammatory cytokines.

For moderate and severe TBI, it is known that the resultant triggered inflammatory cascades and vascular dysruption result in cell death and neuronal dysfunction[17–20]; however, less is known about the ''mild'' forms of TBI. The diversity of clinical outcomes associated with mTBI and the diffuse nature of the injuries classified as mTBI would suggest that no single animal model of mTBI is likely to match 100% of the spectrum of mechanisms and outcomes that have been documented for clinical mTBI.[38] We chose a rodent model that fits many of the clinical observations that characterize mTBI as a useful tool to increase our understanding that the rodent model of mTBI, relying on a 1-atm LFP, would also provide a platform for the development and assessment of intervention strategies for the rational design of clinical therapies.

As a first step in our characterization of a rat mLFP injury model, we chose to use the righting reflex response time as an analog of return of consciousness time interval in humans, an accepted index of TBI severity, because it reflects the time of return of consciousness in the rat.[39,40] Comparison with sham-treated rats allows extrapolating the effects of anesthesia and handling alone; sham-treated rats display righting reflex response times under 4 min, as compared to righting reflex response times between 4 and 10 min, and thus represent a normalizing measure that is useful as a validating tool given the broad range of interanimal variabilty in behavioral and cognitive responses to brain injury. These differences may also reflect the known variability in outcomes present in a clinical setting. We were able to show

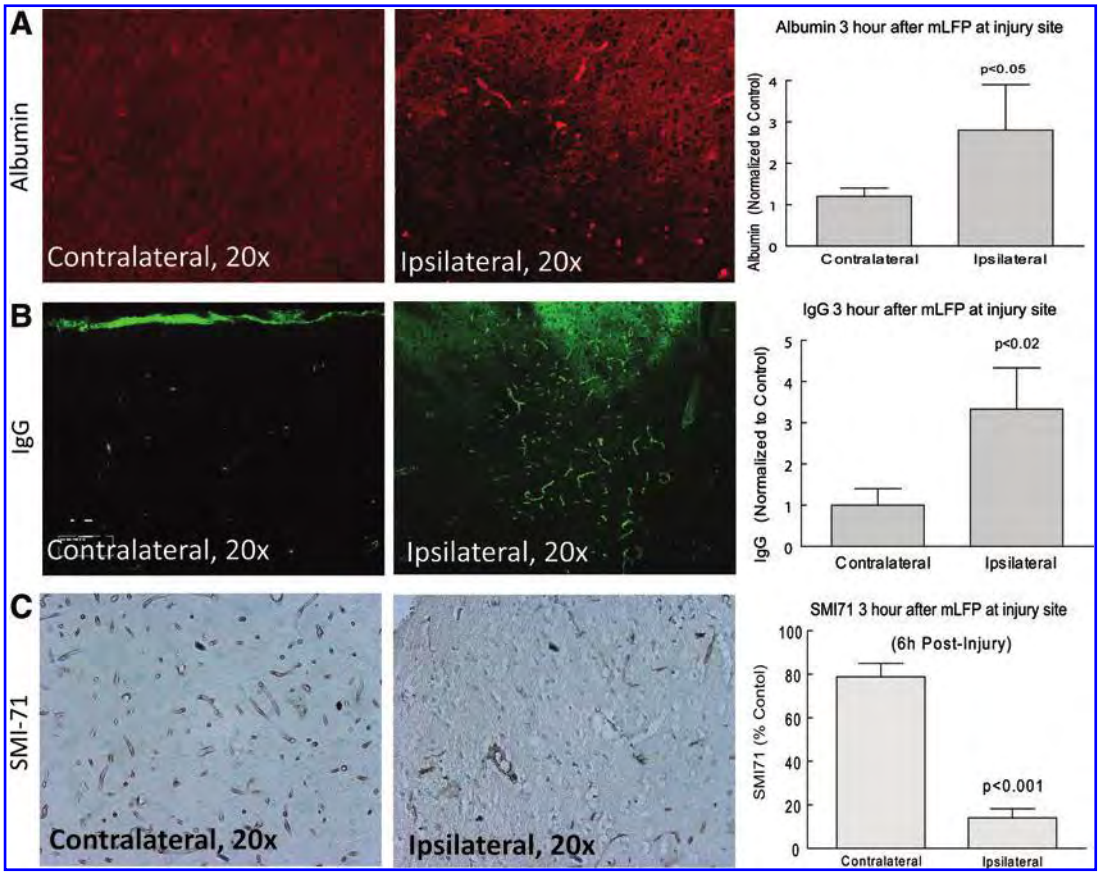

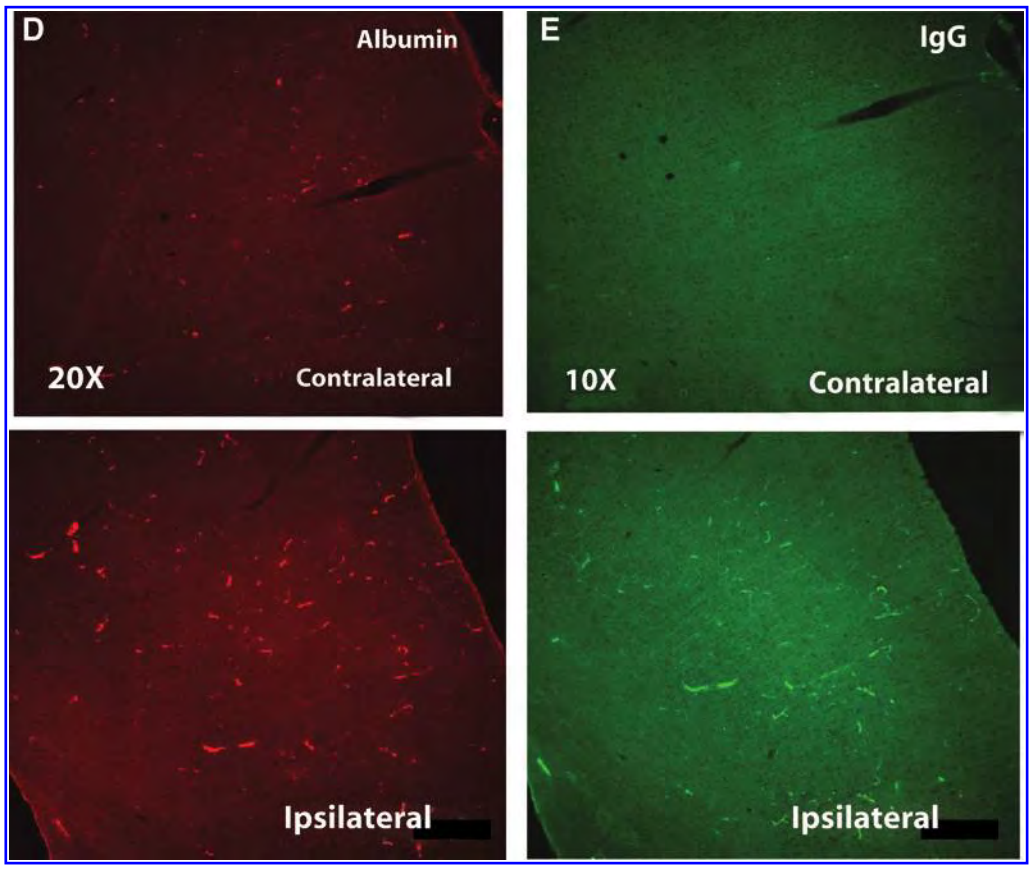

FIG. 6. Immunostaining of **(A)** ALB, **(B)** IgG, and **(C)** SMI-71 3 or 6 h after 1-atm mLFP injury in parietal cortex (original magnification, 20×). Quantitation of cortical **(A)** ALB^+, **(B)** IgG^+, and **(C)** $SMI71^+$ cells after mLFP injury ($p < 0.05$). Representative images in the parietal cortex of **(D)** ALB, **(E)** IgG, and thalamic **(F)** SMI-71 immunostaining 18 days after 1-atm mLFP injury (original magnification, 20×). SMI-71 colocalized with blood vessels, as evidenced by RECA immunostaining. Color image is available online at www.liebertpub.com/neu

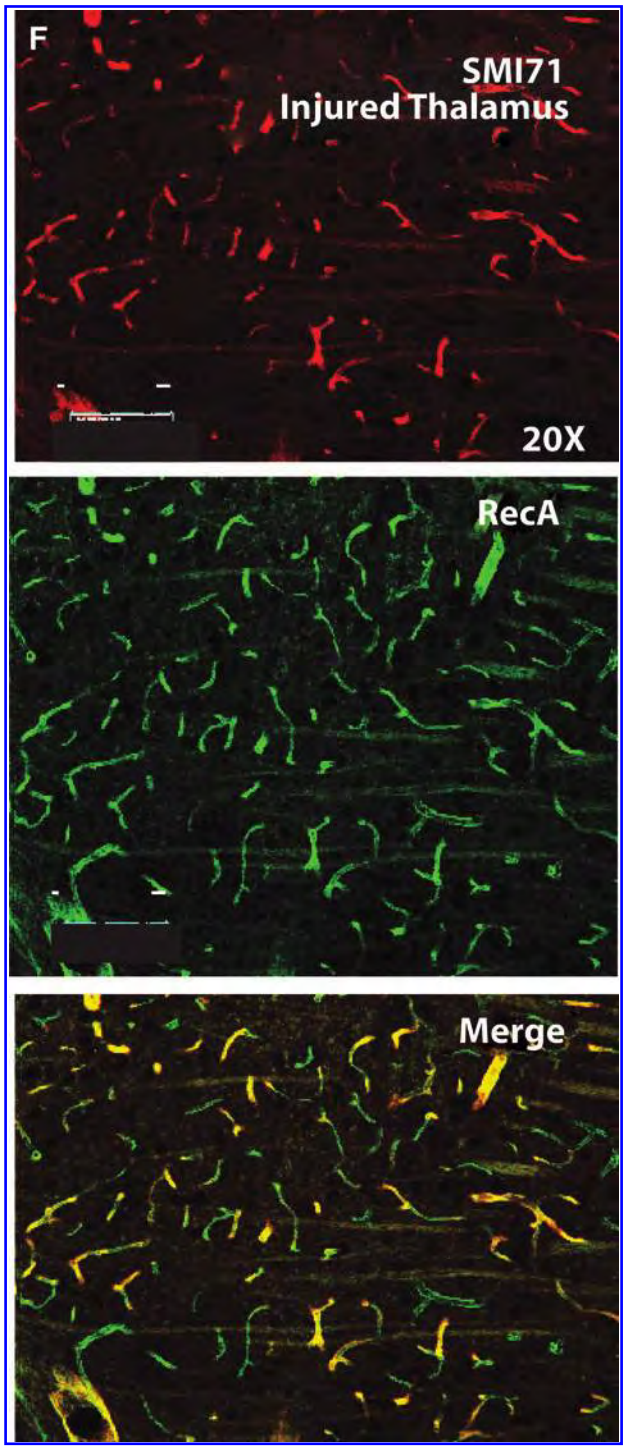

FIG. 6. (Continued).

correlative increases in length of righting reflex response times as a function of mLFP impact severity when measured in atmospheres of pressure (Fig. 1). This allowed us to define a 1-atm pressure injury as our standard for the model.

We also relied on two standard outcome measures of severity of injury by measuring vestibulomotor function as assessed with the beam balance performance test over a defined time interval[32] and number of foot faults on a beam with defined parameters.[33] Exposure to mLFP injury resulted in a significant impairment in locomotor coordination and balance at 11 days postlesion for both these tests (Fig. 2). These results were consistent with the assessment that though delays in righting reflex response times and impairment of beam balance performance and foot fault evaluations indicated a significant impairment associated with mLFP injury (1 atm), they were not as robust as those witnessed by us after 2- and 2.4-atm LFP injuries.

There is evidence of significant increases in inflammatory cytokines in the parenchyma of patients after severe TBI[5,41,42] and in various brain regions in experimental LFP injury,[3] as well as other rodent models of CNS injury.[8–16] The most consistent finding was an increase in IL-1β and TNF-α cytokines and the observation that manipulations that decrease levels of both these cytokines result in improved outcomes.[13,14,43] Here, we report that analyses of three brain regions at 3–6 h after mLFP injury resulted in a robust increase in both IL-1α and in IL-1β as well as TNF-α protein levels, when compared to other known cytokines. Though there were significant increases in IL-6 and GM-CSF in the hippocampus, their very low levels, compared to IL-1α/β and TNF-α levels, would suggest that their role may not be critical after mTBI. Interestingly, there was also an increase in IL-10 at 6 h, consistent with its demonstrated response in moderate or severe TBI.[3] IL-10 is an anti-inflammatory cytokine that has been shown to increase locally after both TBI and spinal cord injury (SCI).[44–49] Attempts to increase IL-10 levels in SCI as a potential therapeutic agent have yielded mixed results.[50,51]

The early increases in IL-1 and TNF-α in the ipsilateral parietal cortices, when compared to their contralateral counterparts, were significant as early as 3 h after mLFP injury. By 6 h, there were also significant increases in IL-1α, IL-1β, TNF-α, IL-6, and IL-10 as well. Increases in IL-1β were the most prominent, relative to the changes in all the other cytokines. In the ipsilateral injured hippocampi, there were significant increases in levels of IL-1α, IL-1β, TNF-α, and IL-6 as early as 3 h after mLFP injury, when comparing ipsilateral to contralateral hemispheres; by 6 h, there were also significant increases in IL-1α, IL-1β, TNF-α, IL-6, and IL-10 as well. Again, increases in IL-1β were the most prominent, relative to the changes for all the other cytokines. In the ipsilateral injured thalami, only IL-1β showed significant increases at 6 h after mLFP injury, when comparing ipsilateral to contralateral hemispheres. Thus, the highest levels were present in the hippocampus and cortex, with thalamic levels being approximately 25% of those in the ipsilateral hippocampi and cortices.

Local IL-1β increases in the CNS are common to most CNS experimental trauma and ischemic injury models. Both IL-1β and IL-1α bind and activate the IL-1 receptor (IL-1R) that, in turn, activate the nuclear factor kappa B transcription factor, followed by increased transcription of cyclooxegenase-2 and inducible nitric oxide (NO) synthase, resulting in increased levels of reactive oxygen species (ROS) and nitrogen oxygen species. The latter, in turn, stimulate lipid peroxidation, DNA damage, and mitochondrial- and endoplasmic reticulum–mediated cell death by apoptosis, necrosis, and autophagy. A number of experimental TBI studies have shown that the resultant damage to the site of injury and hippocampus area are likely to be a major determinant of cognitive impairments associated with TBI.[52–55]

When we determined the cellular origin of cytokines as early as 6 h after mLFP injury, we focused on IL-1β and used confocal IHC, together with a standard cell marker for inflammation. Against a background of very few IL-1β^+-labeled cells in uninjured or

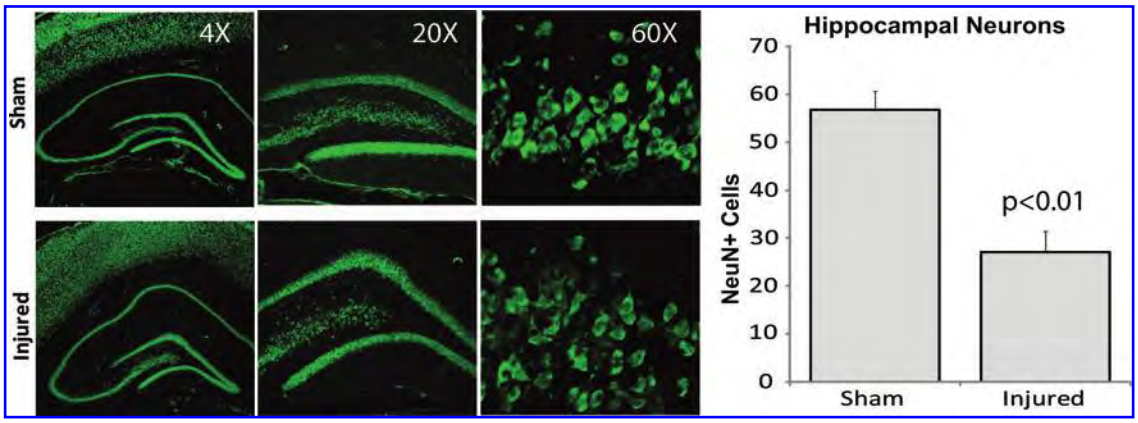

FIG. 7. Immunostaining of NeuN$^+$ cells in hippocampus 18 days after mLFP injury. Representative hippocampal images from mLFP-injured rats after 18 days immunolabeled with NeuN (original magnification, 4×, 20×, and 60×, compared to sham-treated rats. Quantitation of NeuN$^+$ cells: $p<0.01$. Color image is available online at www.liebertpub.com/neu

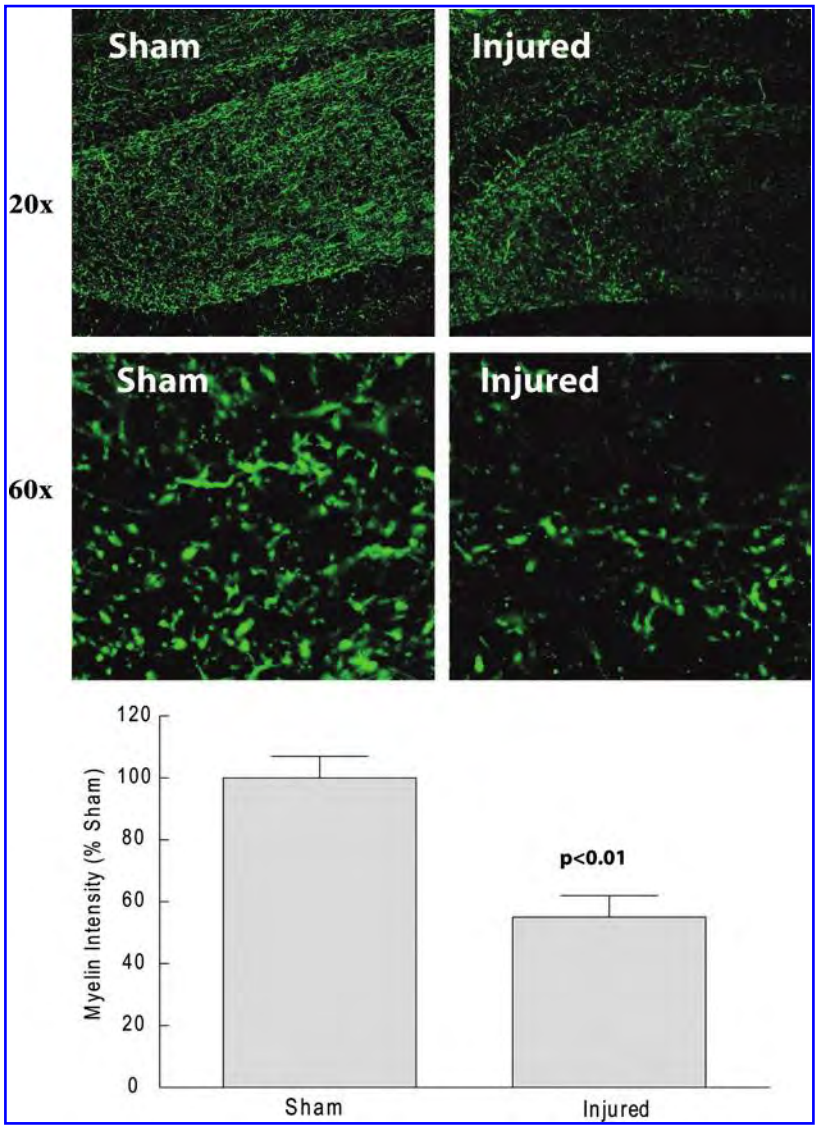

FIG. 8. Immunostaining of MBP$^+$ cells in hippocampus 18 days after mLFP injury. Representative hipppocampal images of mLFP-injured rats after 18 days immunolabeled with MBP (original magnification, 10×; $p<0.01$). Color image is available online at www.liebertpub.com/neu

sham-treated rat brain tissues, the mLFP injured rat brain displayed a significant increase in IBA1$^+$ cells, consistent with reports of IL-1β and TNF-α production by microglia after TBI.[56] Although an increase in IL-1 β^+-activated microglia is consistent with their having a microglial role in subsequent pathology in mTBI, it does not preclude that BBB perturbation may also result, in part, from astroglial activation, macrophage activation, monocyte infiltration, or perturbation of water flux regulation-mediated endothelial responses.

There are both clinical and experimental data that show increased levels of GFAP after severe TBI, reflecting the downstream activation of astrocytes by cytokine-induced inflammation after TBI.[57,58] Two other useful markers for astrocytic activation after TBI are nestin and vimentin.[59,60] Nestin and vimentin are intermediate filament proteins coexpressed by GFAP-positive astrocytes shown to promote scarring and glial proliferation, both of which have detrimental effects on neuronal recuperative and regenerative potential.[61,62] There were significant increases in GFAP immunoreactivity after 6 h and persisting up to 18 days after mLFP injury, reflecting increased astrocytic activation in the cortex, hippocampus, and thalamus ipsilateral to the injury site (Fig. 5). The GFAP$^+$ astrocytes displayed the star-like hypertrophied configuration associated with astrocytes responding to injury that, in part, defines astrocytic activation. mLFP injury induced significant increases in nestin and vimentin labeling of activated astrocytes. These results suggest that mTBI acute injury triggers a cascade of inflammatory local signaling associated with known astrocytic post-trauma pathology that is likely to involve BBB functional impairment and neuronal recuperative processes.

Astrocytes are classically thought to play roles in the regulation of extracellular concentrations of water, potassium and other ions, and glutamate and other transmitters and provide for general homeostasis in the extracellular and synaptic spaces through energy-dependent uptake mechanisms. Specialized processes of astrocytes also play roles in the BBB by end-feet apposition to endothelium of the vasculature in the brain. Microglia are classically thought to be principally phagocytes that are able to be mobilized after injury, infection, disease, and in seizures. When activated, glial cells are known to hypertrophy, increase production of GFAP and proinflammatory cytokines, ROS, adenosine triphosphate, excitatory amino acids, and NO.[63–66] These downstream increases are candidates that can elicit changes in hyperexcitability, affecting sensory function. Additionally, chronically activated astrocytes can lead to permanent blood/spinal cord barrier breakdowns that ensure continued immune cell infiltration and feed-forward continued inflammatory signaling.[67]

In the mammalian system, we propose that normal glial function becomes abnormal and dysfunctional after CNS injury and that the dysfunctional glial state contributes to conditions that initiate and ensure persistence of neuronal dysfunction. Though the concept of glia-neuronal and neuronal-glial interactions were described in invertebrate systems several decades ago,[68,69] the conceptual basis of dysfunctional glial cells contributing to changes in neuronal intracellular signaling and membrane properties is relatively new.[67,70–73] We propose the term ''gliopathy'' to describe the dysfunctional and maladaptive response of glial cells to neural injury. We hypothesize that the initiation of gliopathy after neural injury is the sudden increase in the extracellular concentration of glutamate after nerve or CNS injury[74] that, in some cases, is 37-fold higher than resting concentrations and results in excitotoxicity[75] and glutamate receptor-mediated sensitization of both neuronal and glial populations.[76,77]

Given the robust response of inflammatory signals to mLFP injury, we determined acute effects on BBB integrity, whose role is to isolate CNS tissue from circulating cytokines and immune-like cells. Severe TBI has been shown to disrupt the BBB, as determined by a number of criteria.[37] Measuring the BBB breakdown-mediated intrusion of the blood-derived molecules, ALB and IgG, into the parenchyma as early as 6 h after mLFP injury also showed their significant increase, consistent with an acute impairment of the BBB. Whereas ALB and IgG IHC will indicate the presence of protein infiltration, it will not determine whether that leakage is active or whether it occurred at an earlier time point. The significant mLFP-induced decrease in EBA protein levels, measured using SMI-71, is evidence of deterioration in the BBB, a conclusion based on the known association of decreased EBA with CNS injury resulting in BBB impairment, and the observation that after treatment with Abs to EBA there is an induction of BBB impairment.[78,79] Impairment of the BBB after mLFP injury would suggest that there are likely to be further downstream inflammatory signaling elements that would account for the long-term functional impairments associated with mTBI in the clinical context.

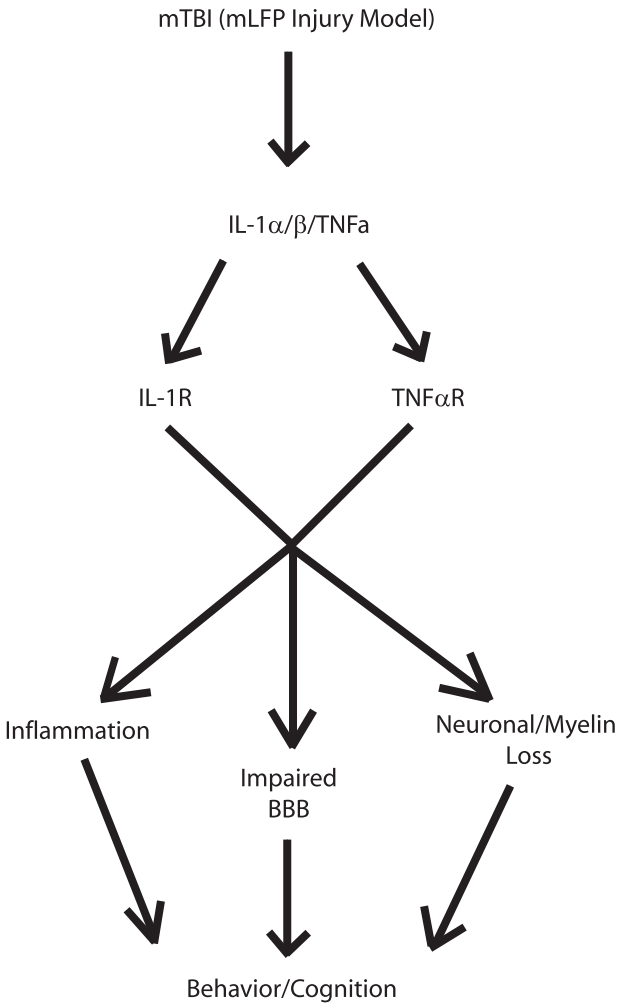

FIG. 9. Proposed mTBI-triggered inflammatory cascade. mTBI stimulates increased levels of IL-1α/β and TNF-α that, in turn, activate early robust inflammatory signaling by monocyte and glial activation, BBB impairment, and eventual neuronal and glial loss that are likely to affect behavior and cognition.

One potential contributor to the persistent inflammatory responses to mLFP injury could be continued BBB disruption and resultant increased BBB dysfunction-associated increased permeability. To confirm the published literature on increased BBB permeability after mTBI (the bulk of that literature addresses moderate TBI and/or stroke),[20,37] we also assessed the presence of blood-borne proteins in the brain at 18 days post-trauma. When we stained for ALB and IgG and compared results between naïve and injured, there was a qualitatively very definitive presence of blood-borne proteins in the injured brains at 18 days postinjury (Fig. 6), clearly documenting BBB impairment up to 18 days postinjury. This is important from the perspective of being able to introduce therapeutic proteins in the injured brain, because agents thought to be impermeable in uninjured brains would have access to the postinjury brain parenchyma.

Whereas ALB IHC will indicate the presence of ALB at different time points, it will not determine whether that leakage is active or whether it occurred at an earlier time point. EBA passage into CNS tissue indicates an actively leaky barrier. Finally, we also showed a decreased appearance of EBA, a marker for BBB integrity.[78,79] The resulting mTBI-induced decrase in EBA expression is indicative of BBB dysfunction, a conclusion based on the known association of decreased EBA with CNS injury resulting in BBB impairment and induction of BBB impairment after treatment with Abs to EBA.[78,79]

We characterized BBB function by measuring levels of serum ALB in the parietal cortex 18 days after mLFP injury. As shown in Figure 6, there was more than a 2-fold increase in ALB in the ipsilateral parietal cortex, as compared to control hemisphere, 18 days after mLFP injury. Not surprisingly, there was also a 3-fold increase in IgG at the same site, consistent with an impaired BBB (Fig. 6). An indicator of BBB function is SMI-71. When SMI-71 was measured 18 days after injury, there was a decrease in SMI-71 levels colocalized to the endothelial lining of blood vessels, as shown by colocalization with the RECA endothelial marker, consistent with impaired BBB functionality (Fig. 6). This provides good evidence for the involvement of impaired vascular function after mTBI, which would be consistent with chronic low-level inflammatory events and which, because of cross-talk with other systems, may explain some of the persistance of behavioral outcomes. Thus, treatments that intervene in inflammatory receptor-mediated downstream pathways would be predicted to preserve neuronal function and, consequently, improve behavioral function.

These results are consistent with mLFP injury triggering a cascade in which the inflammatory cytokines, IL-1α and IL-1β, play a major role in triggering downstream impairment of the BBB and, further, more persistant microglial activation (Fig. 9).

Author Disclosure Statement

No competing financial interests exist.

References

1. Fan, L., Young, P.R., Barone, F.C., Feuerstein, G.Z., Smith, D.H., and McIntosh, T.K. (1996). Experimental brain injury induces differential expression of tumor necrosis factor-alpha mRNA in the CNS. Brain Res. Mol. Brain Res. 36, 287–291.
2. Shohami, E., Ginis, I., and Hallenbeck, J.M. (1999). Dual role of tumor necrosis factor alpha in brain injury. Cytokines Growth Factors Rev. 10, 119–130.
3. Knoblach, S.M., and Faden, A.I. (1998). Interleukin-10 improves outcome and alters proinflammatory cytokine expression after experimental brain injury. Exp. Neurol. 153, 143–151.
4. Knoblach, S. M., and Faden, A.I. (2000). Cortical interleukin-1 beta elevation after traumatic brain injury in the rat: no effect of two selective antagonists on motor recovery. Neurosci. Lett. 289, 5–8.
5. Taupin, V., Toulmond, S., Serrano, A., Benavides, J., and Zavala, F. (1993). Increase in IL-6, IL-1, and TNF levels in rat brain following lesion. Influence of pre- and post-traumatic treatment with peripheral-type (p site) benzodiazepine ligand. J. Neuroimmunol. 42, 177–185.
6. Fan, L., Young, P.R., Barone, F.C., Feuerstein, G.Z., Smith, D.H., and McIntosh, T.K. (1995). Experimental brain injury induces expression of interleukin-1 beta mRNA in the rat brain. Brain Res. Mol. Brain Res. 30, 125–130.
7. Shohami, E., Gallily, R., Mechoulam, R., Bass, R., and Ben-Hur, T. (1997). Cytokine production in the brain following closed head injury: dexanabinol (HU-211) is a novel TNF-alpha inhibitor and an effective neuroprotectant. J. Neuroimmunol. 72, 169–177.
8. Akuzawa, S., Kazui, T., Shi, E., Yamashita, K., Bashar, A.H., and Terada, H. (2008). Interleukin-1 receptor antagonist attenuates the severity of spinal cord ischemic injury in rabbits. J. Vasc. Surg. 48, 694–700.
9. Banwell, V., Sena, E.S., and Macleod, M.R. (2009). Systematic review and stratified meta-analysis of the efficacy of interleukin-1 receptor antagonist in animal models of stroke. J. Stroke Cerebrovasc. Dis. 18, 269–276.
10. Baratz, R., Tweedie, D., Rubovitch, V., Luo, W., Yoon, J.S., Hoffer, B.J., Greig, N.H., and Pick, C.G. (2011). Tumor necrosis factor-alpha synthesis inhibitor, 3,6'-dithiothalidomide, reverses behavioral impairments induced by minimal traumatic brain injury in mice. J. Neurochem. 118, 1032–1042.
11. Brochu, M.E., Girard, S., Lavoie, K., Sebire, G. (2011). Developmental regulation of the neuroinflammatory responses to LPS and/or hypoxia-ischemia between preterm and term neonates: an experimental study. J. Neuroinflamm. 8, 55.
12. Dinarello, C.A. (2011). A clinical perspective of IL-1beta as the gatekeeper of inflammation. Eur. J. Immun. 41, 1203–1217.
13. Fabian, R.H., Perez-Polo, J.R., and Kent, T.A. (2004). Extracellular superoxide concentration increases following cerebral hypoxia but does not affect cerebral blood flow. Int. J. Dev. Neurosci. 22, 225–230.
14. Hu, X., Nesic-Taylor, O., Qiu, J., Rea, H.C., Fabian, R., Rassin, D.K., and Perez-Polo, J.R. (2005). Activation of nuclear factor-κB signaling pathway by interleukin-1 after hypoxia/ischemia in neonatal rat hippocampus and cortex. J. Neurochem. 93, 26–37.
15. Nesic, O., Svrakic, N., Xu, G.-Y., McAdoo, D., Westlund, K.N., Hulsebosch, C.E., Ye, Z., Galante, G., Soteropoulos, P., Tolias, P., Young, W., Hart, R.P., and Perez-Polo, J.R. (2002). DNA microarray analysis of the contused spinal cord: effect of NMDA receptor inhibition. J. Neurosci. Res. 68, 406–423.
16. Tuttolomondo, A., Di Raimondo, D., di Sciacca, R., Pinto, A., and Licata, G. (2008). Inflammatory cytokines in acute ischemic stroke. Curr. Pharm. Des. 14, 3574–3589.
17. Conti, A.C., Raghupathi, R., Trojanowski, J.Q., and McIntosh, T.K. (1998). Experimental brain injury induces regionally distinct apoptosis during the acute and delayed post-traumatic period. J. Neurosci. 18, 5663–5672.
18. Xiong, Y., Shie, F.-Y., Zhang, J., Lee, C.-P., and Ho, Y.-S. (2004). The protective role of cellular glutathione peroxidase against trauma-induced mitochondrial dysfunction in the mouse brain. J. Stroke Cerebrovasc. Dis. 13, 129–137.
19. Israelsson, C., Bengsston, H., Kylberg, A., Kullander, K., Lewen, A., Hillered, L., and Ebendal, T. (2008). Distinct cellular patterns of upregulated chemokine expression supporting a prominent inflammatory role in traumatic brain injury. J. Neurotrauma 25, 959–974.
20. Donkin, J.J., Nimmo, A.J., Cernak, I., Blumbergs, P.C., and Vink, R. (2009). Substance P is associated with the development of brain edema and functional deficits after traumatic brain injury. J. Cereb. Blood Flow Metab. 29, 1388–1398.
21. Frugier, T., Morganti-Kossmann, M.C., O'Reilly, D., and McLean, C.A. (2010). *In situ* detection of inflammatory mediators in post mortem human brain tissue after traumatic injury. J. Neurotrauma 27, 497–507.
22. Cantu, R.C. (2007). Chronic traumatic encephalopathy in the National Football League. Neurosurgery 61, 223–225.

23. Department of Veterans Affairs and Department of Defense. (2009). Clinical practice guideline: management of concussion/mild traumatic brain injury. Available at: www.healthquality.va.gov/mtbi/concussion_mtbi_full_1_0.pdf. Accessed November 15, 2010.
24. Okie, S. (2005). Traumatic brain injury in the war zone. N. Engl. J. Med. 352, 2043–2047.
25. Omalu, B.I, DeKosky, S.T., Hamilton, R.L., Minster, R.L., Kamboh, M.I., Shakir, A.M., and Wecht, C.H. (2006). Chronic traumatic encephalopathy in a national football league player: part II. Neurosurgery 59, 1086–1092.
26. Riggio, S. (2011). Traumatic brain injury and its neurobehavioral sequelae. Neurolog. Clin. 29, 35–47.
27. Schultz, B.A., Cifu, D.X., McNamee, S., Nichols, M., and Carne W. (2011). Assessment and treatment of common persistent sequelae following blast induced mild traumatic brain injury. NeuroRehabilitation 28, 309–320.
28. Shukla, D., Devi, B.I., and Agrawal, A. (2011). Outcome measures for traumatic brain injury. Clin. Neurol. Neurosurg. 113, 435–441.
29. Dixon, C.E., Lyeth, B.G., Povlishock, J.T., Findling, R.L., Hamm, R.J., Marmarou, A., Young, H.F., and Hayes R.L. (1987). A fluid percussion model of experimental brain injury in the rat. J. Neurosurg. 67, 110–119.
30. DeWitt, D.S., Smith, T.G., Deyo, D.J., Miller, K.R., Uchida, T., and Prough, D.S. (1997). L-arginine and superoxide dismutase prevent or reverse cerebral hypoperfusion after fluid-percussion traumatic brain injury. J. Neurotrauma 14, 223–233.
31. Thompson, H.J., Lifshitz, J., Marklund, N.,Grady, M.S., Graham, D.I., Hovda, D.A., and McIntosh, T.K. (2005). Lateral fluid percussion brain injury: a 15-year review and evaluation. J. Neurotrauma 22, 42–75.
32. Hamm, R.J. (2001). Neurobehavioral assessment of outcome following traumatic brain injury in rats: an evaluation of selected measures. J. Neurotrauma 18, 1207–1216.
33. Zhang, L., Schallert, T., Zhang, Z.G., Jiang, Q., Arniego, P., Li, Q., Lu, M., and Chopp, M. (2002). A test for detecting long-term sensorimotor dysfunction in the mouse after focal cerebral ischemia. J. Neurosci. Methods 117, 207–214.
34. Cortez, S.C., McIntosh, T.K., Noble, L.J. (1989). Experimental fluid percussion brain injury: vascular disruption and neuronal and glial alterations. Brain Res. 482, 271–282.
35. Latov, N., Nilaven, G., Zimmerman, E.A., Johnson, W.G., Silverman, A.-J., Defendini, R., and Cote, L. (1979). Fibrillary astrocytes proliferate in response to brain injury: a study combining immunoperoxidase technique for glial fibrillary acidic protein and radioautography of tritiated thymidine. Dev. Biol. 72, 381–384.
36. Donkin, J.J., and Vink, R. (2010). Mechanisms of cerebral edema in traumatic brain injury: therapeutic developments. Curr. Opin. Neurol. 23, 293–299.
37. Shlosberg, D., Benifla, M., Kaufer, D., and Friedman, A. (2010). Blood–brain barrier breakdown as a therapeutic target in traumatic brain injury. Nat. Rev. Neurol. 6, 393–403.
38. Laurer, H.L., and McIntosh, T.K. (1999). Experimental models of brain trauma. Curr. Opin. Neurol. 12, 715–721.
39. Alkire, M.T., McReynolds, J.R., Hahn, E.L., and Trivedi, A.N. (2007). Thalamic microinjection of nicotine reverses sevoflurane induced loss of righting reflex in the rat. Anesthesiology 107, 264–272.
40. Nguyen, H.T., Li, K.Y., daGraca, R.L., Delphin, E., Xiong, M., and Ye, J.H. (2009). Behavior and cellular evidence form propofol-induced hypnosis involving brain glycine receptors. Anesthesiology 110, 326–332.
41. Helmy, A., Carpenter, K.L., Menon, D.K., Pickard, J.D., and Hutchinson, P.J. (2011). The cytokine response to human traumatic brain injury: temporal profiles and evidence for cerebral parenchymal production. J. Cereb. Blood Flow Metab. 31, 658–670.
42. Woodroofe, M.N., Sarna, G.S., Wadhwa, M., Hayes, G.M., Loughlin, A.J., Tinker, A., and Cuzner, M.L. (1991). Detection of interleukin-1 and interleukin-6 in adult rat brain, following mechanical injury, by *in vivo* microdialysis: evidence of a role for microglia in cytokine production. J. Neuroimmunol. 33, 227–236.
43. He, J., Evans, C.O., Hoffman, S.W., Oyesiku, N.M., Stein, D.G. (2004). Progesterone and allopregnanolone reduce inflammatory cytokines after traumatic brain injury. Exp. Neurol. 189, 404–412.
44. Ward, J.L., Harting, M.T., Cox, C.S., Jr., and Mercer, D.W. (2011). Effects of ketamine on endotoxin and traumatic brain injury induced cytokine production in the rat. J. Trauma 70, 1471–1479.
45. Li, M., Li, F., Luo, C., Shan, Y., Zhang, L., Qian, Z., Zhu, G., Lin, J., and Feng, H. (2011). Immediate splenectomy decreases mortality and improves cognitive function of rats after severe traumatic brain injury. J. Trauma 71, 141–147.
46. Lee, S.I., Jeong, S.R., Kang, Y.M., Han, D.H., Jin, B.K., Namgung, U., and Kim, B.G. (2010). Endogenous expression of interleukin-4 regulates macrophage activation and confines cavity formation after traumatic spinal cord injury. J. Neurosci. Res. 88, 2409–2419.
47. Tai, P.A., Chang, C.K., Niu, K.C., Lin, M.T., Chiu, W.T., and Lin, C.M. (2010). Attenuating experimental spinal cord injury by hyperbaric oxygen: stimulating production of vasculoendothelial and glial cell line-derived neurotrophic growth factors and interleukin-10. J. Neurotrauma 27, 1121–1127.
48. Zhou, Z., Peng, X., Insolera, R., Fink, D.J., and Mata, M. (2009). IL-10 promotes neuronal survival following spinal cord injury. Exp. Neurol. 220, 183–190.
49. Genovese, T., Esposito, E., Mazzon, E., Di Paola, R., Caminiti, R., Bramanti, P., Cappelani, A., and Cuzzocrea, S. (2009). Absence of endogenous interleukin-10 enhances secondary inflammatory process after spinal cord compression injury in mice. J. Neurochem. 108, 1360–1372.
50. Brambilla, R., Hurtado, A., Persaud, T., Esham, K., Pearse, D.D., Oudega, M., and Bethea J.R. (2009). Transgenic inhibition of astroglial NF-kappa B leads to increased axonal sparing and sprouting following spinal cord injury. J. Neurochem. 110, 765–778.
51. Bethea, J.R., Nagashima, H., Acosta, M.C., Briceno, C., Gomez, F., Marcillo, A.E., Loor, K., Green, J., and Dietrich, WD. (1999). Systemically administered interleukin-10 reduces tumor necrosis factor-alpha production and significantly improves functional recovery following traumatic spinal cord injury in rats. J. Neurotrauma 16, 851–863.
52. Ekmark-Lewen, S., Lewen, A., Meyerson, B.J., Hillered, L. (2010). The multivariate concentric square field test reveals behavioral profiles of risk taking, exploration, and cognitive impairment in mice subjected to traumatic brain injury. J. Neurotrauma 27, 1643–1655.
53. Doll, H., Truebel, H., Kipfmueller, F., Schaefer, U., Neugebauer, E.A., Wirth, S., and Maegele, M. (2009). Pharyngeal selective brain cooling improves neurofunctional and neurocognitive outcome after fluid percussion brain injury in rats. J. Neurotrauma 26, 235–242.
54. Conte, V., Raghupathi, R., Watson, D.J., Fujimoto, S., Royo, N.C., Marklund, N., Stocchetti, N., and McIntosh TK. (2008). TrkB gene transfer does not alter hippocampal neuronal loss and cognitive deficits following traumatic brain injury in mice. Restor. Neurol. Neurosci. 26, 45–56.
55. Reid, W.M., and Hamm, R.J. (2008). Post-injury atomoxetine treatment improves cognition following experimental traumatic brain injury. J. Neurotrauma 25, 248–256.
56. Griffin, W.S., Sheng, J.G., Gentleman, S.M., Graham, D.I., Mrak, R.E., and Roberts, G.W. (1994). Microglial interleukin-1 alpha expression in human head injury: correlations with neuronal and neuritic beta-amyloid precursor protein expression. Neurosci. Lett. 176, 133–136.
57. Nylén, K., Ost, M., Csajbok, L.Z., Nilsson, I., Blennow, K., Nellgård, B., and Rosengren, L. (1996). Increased serum-GFAP in patients with severe traumatic brain injury is related to outcome. J. Neurol. Sci. 240, 85–91.
58. McIntosh, T.K., Juhler, M., and Wieloch, T. (1998). Novel pharmacologic strategies in the treatment of experimental traumatic brain injury: 1998. J. Neurotrauma 15, 731–769.
59. Kaya, S. S., Mahmood, A., Li, Y., Yavuz, E., and Chopp, M. (1999). Expression of nestin after traumatic brain injury in rat brain. Brain Res. 840, 153–157.
60. Ekmark-Lewén, S., Lewén, A., Israelsson, C., Li, G.L., Farooque, M., Olsson, Y., Ebendal, T., and Hillered, L. (2010). Vimentin and GFAP responses in astrocytes after contusion trauma to the murine brain. Restor. Neurol. Neurosci. 28, 311–321.
61. Frisen, J., Jahansson, C.B., Torok, C., Risling, M., and Lendahl, U. (1995). Rapid, widespread, and longlasting induction of nestin contributes to the generation of glial scar tissue after CNS injury. J. Cell Biol. 131, 453–464.
62. Wei, L.-C., Shi, M., Chen, L.-W., Cao, R., Zhang, P., and Chan, Y.S. (2002). Nestin-containing cells express glial fibrillary acidic protein in the proliferative regions of central nervous system of postnatal developing and adult mice. Dev. Brain Res. 139, 9–17.
63. Johnstone, M., Gearing, A.J., and Miller, K.M. (1999). A central role for astrocytes in the inflammatory response to beta-amyloid: chemokines,

cytokines, and reactive oxygen species are produced. J. Neuroimmunol. 93, 182–193.
64. Martin, D.D. (1992). Synthesis and release of neuroactive substances by glia cells. Glia 5, 81–94.
65. Shafer, R.A., and Murphy, S. (1997). Activated astrocytes induce nitric oxide synthase-2 in cerebral endothelium via tumor necrosis factor alpha. Glia 21, 370–379.
66. Tanaka, M., Sotomatsu, A., Yoshida, T., Hirai, S., and Nishida, A. (1994). Detection of superoxide production by activated microglia using a sensitive and specific chemiluminescence assay and microglia-mediated PC12h cell death. J. Neurochem. 63, 266–270.
67. Nesic, O., Lee, J., Johnson, K.M., Ye, Z., Xu, G.-Y., Unabia, G.C., Wood, T.G., McAdoo, D.J., Westlund, K.H., Hulsebosch, C.E., and Perez-Polo, J.R. (2005). Transcriptional profiling of spinal cord injury-induced central neuropathic pain. J. Neurochem. 95, 998–1014.
68. Lasek, R.J., Gainer, H., and Przybylski, R.J. (1974). Transfer of newly synthesized proteins from Schwann cells to the squid giant axon. Proc. Natl. Acad. Sci. U. S. A. 71, 1188–1192.
69. Villegas, J. (1972). Axon-Schwann cell interaction in the squid nerve fibre. J. Physiol. 225, 275–296.
70. Crown, E.D., Gwak, Y.S., Ye, Z., Johnson, K.M., and Hulsebosch, C.E. (2008). Activation of p38 MAP kinase is involved in central neuropathic pain following spinal cord injury. Exp. Neurol. 213, 257–267.
71. Detloff, M.R., Fisher, L.C., McGaughy, V., Longbrake, E.E., Popovich, P.G., and Basso, D.M. (2008). Remote activation of microglia and pro-inflammatory cytokines predict the onset and severity of below-level neuropathic pain after spinal cord injury in rats. Exp. Neurol. 212, 337–347.
72. DeLeo, J.A., Tawfik, V.L., and LaCroix-Fralish, M.L. (2006). The tetrapartite synapse: path to CNS sensitization and chronic pain. Pain 122, 17–21.
73. Gwak, Y.S., Crown, E.D., Unabia, G.C., and Hulsebosch, C.E. (2008). Propentofylline attenuates allodynia, glial activation, and modulates GABAergic tone after spinal cord injury in the rat. Pain 138, 410–422.
74. McAdoo, D.J., Xu, G-Y., Robak, G., and Hughes, M.G. (1999). Changes in amino acid concentrations over time and space around an impact injury and their diffusion through the rat spinal cord. Exp. Neurol. 159, 538–544.
75. Xu, G.-Y., Liu, S., Hughes, M.G., and McAdoo, D.J. (2008). Glutamate-induced losses of oligodendrocytes and neurons and activation of caspase-3 in the rat spinal cord. Neuroscience 153, 1034–1047.
76. Hulsebosch, C.E. (2005). From discovery to clinical trials: treatment strategies for central neuropathic pain after spinal cord injury. Curr. Pharm. Des. 11, 1411–1420.
77. Hulsebosch, C.E. (2008). Gliopathy ensures persistent inflammation and chronic pain after spinal cord injury. Exp. Neurol. 214, 6–9.
78. Lu, H., Demny, S., Zuo, Y., Rea, W., Wang, L., Chefer, S.I., Vaupel, D.B., Yang, Y., and Stein, E.A. (2010). Temporary disruption of the rat blood–brain barrier with a monoclonal antibody: a novel method for dynamic manganese-enhanced MRI. Neuroimage 50, 7–14.
79. Sköld, M.K., Von Gertten, C., Sandberg-Nordqvist, A-C,. Mathiesen, T., and Holmin, S. (2005). VEGF and VEGF receptor expression after experimental brain contusion in rat. J. Neurotrauma 22, 353–367.

Address correspondence to:
J. Regino Perez-Polo, PhD
Department of Biochemistry and Molecular Biology
The University of Texas Medical Branch
301 University Boulevard
Galveston, TX 77555

E-mail: regino.perez-polo@utmb.edu